

# **UNIVERSITA' DEGLI STUDI DI PARMA**

Dottorato di ricerca in Progettazione e sintesi di composti  
biologicamente attivi

Ciclo XXV

## **Interfering with the excitatory amino acids signalling in the brain for the design of novel neuroprotective agents**

Coordinatore:

Chiar.mo Prof. Marco Mor

Tutor:

Chiar.mo Prof. Gabriele Costantino

Dottorando: Gian Paolo Vallerini



## SUMMARY

<b>Section 1. INTRODUCTION.....</b>	<b>1</b>
<b>Section 2. GLUTAMIC ACID .....</b>	<b>3</b>
2.1. Pharmacology of glutamic acid in the CNS .....	3
2.2. Clinical relevance of glutamatergic system .....	9
<b>Section 3. KYNURENINE PATHWAY.....</b>	<b>12</b>
3.1. Overview .....	12
3.2. Neuroactive kynurenines.....	16
3.3. Kynurenine pathway related pathologies.....	18
<b>Section 4. AIM OF THE WORK .....</b>	<b>22</b>
4.1. 3-Hydroxyanthranilic acid 3,4-dioxygenase .....	23
4.2. State of the art of 3-HAO inhibitors .....	27
4.3. Design of novel pyridine N-oxide based 3-HAO inhibitors.....	29
<b>Section 5. RESULTS AND DISCUSSION.....</b>	<b>31</b>
5.1. In vitro 3-HAO inhibition.....	31
5.2. SAR.....	36
5.3. In vivo tests .....	37
5.4. Chemistry .....	40
<b>Section 6. CONCLUSIONS AND FUTURE PERSPECTIVES .....</b>	<b>48</b>
<b>Section 7. EXPERIMENTAL SECTION (I) .....</b>	<b>52</b>
7.1. Materials and methods .....	52
7.2. Synthetic procedures and characterization of products .....	54
<b>Section 8. DIAZO CHEMISTRY .....</b>	<b>66</b>
8.1. Synthesis of amino acids .....	67
8.2. Lewis acid-induced decomposition of $\alpha$ -diazo- $\beta$ -hydroxyesters.....	70
8.3. $BF_3 \cdot Et_2O$ -induced decomposition of 2-diazo-3-hydroxy-3-phenyl-3-alkylpropanoates in acetonitrile .....	73

<b>Section 9. EXPERIMENTAL SECTION (II)</b> .....	<b>82</b>
<i>9.1. Materials and methods</i> .....	82
<i>9.2. Synthetic procedures</i> .....	83
<b>References</b> .....	<b>85</b>

## Section 1. INTRODUCTION

Amino acids are one of the most important classes of molecules for life on Earth: they are the bricks that all the biological systems, from simple prokaryotes to highly evolved mammals, utilize to build proteins, following the essential “assembly instructions” included in nucleic acids.

Additionally, amino acids as themselves are also responsible for a wide array of fundamental biological functions. One over all, they play crucial roles in intercellular signalling, both in periphery and in the central nervous system (CNS), in superior organisms.

Besides the well-known relevance of amino acids in proteins biosynthesis and their dietary essentiality, the regulatory activities that they exert in the control of vital physiological processes, primarily in the brain, has become a critical object of study, and fine tuning of this kind of regulatory system is now one of the main challenges in the drug discovery research of neurological diseases.

GABA-ergic and glutamat-ergic systems are of special importance in the human brain, particularly for the correct outcome of crucial functions, such as growth and assembly of the neuronal web, that are tightly related to cognitive functioning and to learning and memory. In adult life, the homeostasis of the whole CNS is also maintained by the two neurotransmitters responsible for these regulatory networks, 4-aminobutirric acid (GABA), a  $\gamma$ -amino acid endowed with inhibitory activity on the neurotransmission, and glutamic acid (Glu), an  $\alpha$ -amino acid, the principal excitatory agent of the CNS. GABAergic drugs are nowadays consolidated treatments of choice for a variety of psychiatric

and neurological disorders, such as anxiety, epilepsy and neuropathic pain, while glutamatergic agents are not yet available in a clinically useful way (except for a limited number of examples, that will be discussed in the following sections), although a lot of evidences unequivocally confirm implications of Glu in both the onset and the progression of a wide spectrum of neuropathological conditions, above all those commonly referred to as neurodegenerative diseases.

The main objectives of the present work were to discover novel pharmacological tools useful to study the effect of interfering with Glu-related excitatory transmission in chronic conditions in which a tight relationship between over-activation of glutamatergic signalling and neuronal death seems to exist, such as in Huntington's disease (HD). In the following pages, after discussing the relevance of Glu in the CNS, with a focus on therapeutic usefulness of exogenous glutamatergic transmission modulators, the work that led to the drafting of this thesis, its scope, aim, rationale and results obtained will be presented in detail.

Sections 8 and 9 are dedicated to a pure organic chemistry work, that I carried on during the second year of my doctorate at the Dipartimento di Chimica e Tecnologia del Farmaco - Università di Perugia, in collaboration with Prof. Roberto Pellicciari's research group, in which I explored the Lewis acid-induced decomposition of  $\alpha$ -diazo- $\beta$ -hydroxyesters in acetonitrile, a reaction that has proven to be a powerful method for the one-pot synthesis of highly diversified  $\alpha$ -,  $\beta$ - and  $\gamma$ -amino acids precursors.

## Section 2. GLUTAMIC ACID

### 2.1. Pharmacology of glutamic acid in the CNS

L-Glutamic acid is the principal excitatory neurotransmitter in the central nervous system. Glutamatergic transmission is present in all brain districts and is crucial at every level of cerebral functions. Typical characteristics of superior organisms, such as the mechanisms underlying the development of memory and neuronal plasticity, are regulated by Glu which, acting on specific receptors, explicates its regulatory activity mainly by modulating the release of other neurotransmitters along synaptic pathways and by contributing to the cell survival.<sup>1-3</sup>

Glu, which is synthesized in the nerve terminals from glutamine, by glutaminase or from  $\alpha$ -ketoglutarate, by glutamate dehydrogenase, is stored in presynaptic vesicles and, after a depolarization event, is released in the synaptic space in high concentrations, where it activates excitatory postsynaptic receptors, but also modulates presynaptically the release of other neurotransmitters, in particular GABA from GABAergic neurons.<sup>4</sup> This modulation is also exerted in a feed-back fashion, on the presynaptic, glutamate-releasing neuron. A system of transporters for excitatory amino acids (EAATs) is responsible for the rapid re-uptake of Glu from the synapse, to both glial cells and neurons, where, respectively, Glu is re-converted into glutamine or accumulated in the nerve terminal vesicles by specialized transporters (VGLUTs). Glutamine synthesized in glia is then transferred to glutamatergic neurons, where it is re-converted into Glu, establishing the correct homeostasis of Glu pool (Figure 1).

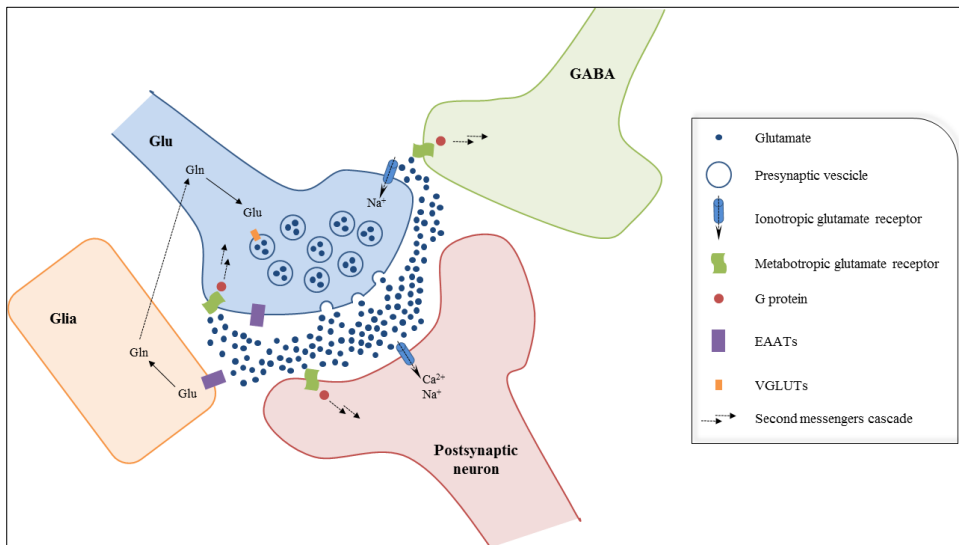


**Figure 1.** Schematic representation of a glutamatergic synapse. **Glu:** glutamate-releasing neuron; **GABA:** GABA-releasing neuron; **Glia:** glial cell; **Glu:** glutamate; **Gln:** glutamine.

Dysregulations in the glutamatergic transmission are of particular therapeutic interest, as well as abnormal, Glu-mediated cellular excitability, found in several neurodegenerative diseases, is the last downstream cause of neuronal and glial death.<sup>5,6</sup> This deleterious potential which Glu is responsible for, is known with the name of excitotoxicity. On the other hand, hypo-glutamatergic functioning is also related to non-physiological conditions, e. g. cognitive deficits and mood disorders.

Characterization of Glu receptors, which are responsible for all the physiological functions, as well as for the pathological consequences of impaired glutamatergic transmission, excitotoxicity *in primis*, is certainly a crucial issue for glutamate research, especially to define clinically useful strategies. During the second half of the last century, great efforts have been dedicated to the understanding of the molecular basis of glutamatergic transmission in the brain.<sup>1</sup> It soon became clear that the actions of Glu are the result of the activation of different receptors and, thanks to the discovery of specific agonists and antagonists, a wide,



systematic characterization of the “extended family” of glutamate receptors is now available.<sup>7,8</sup>

A brief description of the updated knowledge about Glu receptors is here reported. Glu, as a neurotransmitter, explicates its actions through the activation of both ionotropic and metabotropic receptors, which are expressed in the synapses throughout the whole brain.

### Ionotropic receptors

Ionotropic glutamate receptors belong to the family of the “ligand-gated ion channels”. They are responsible for the intake of cations, mainly  $\text{Ca}^{2+}$ , but also  $\text{Na}^{+}$ , in glutamate-stimulated neuronal cells. Increase in the intracellular concentrations of cations causes depolarization and neuron activation, resulting in physiological responses, depending on the type of the excited neuron.

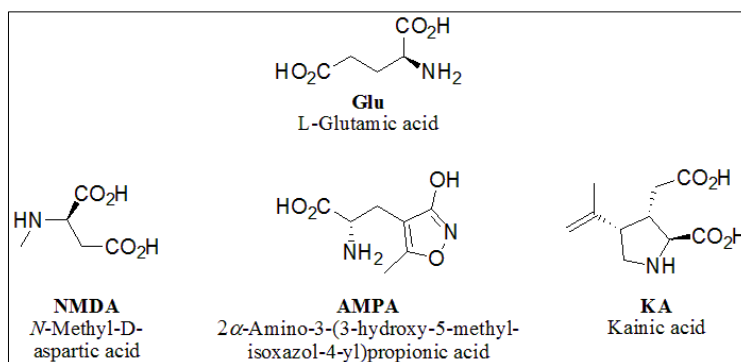


**Figure 2.** Comparison between Glu and selective agonists of its ionotropic receptors.

Three classes of glutamate-gated ion channels are known, NMDA (*N*-methyl-D-aspartate), AMPA [*2α*-amino-3-(3-hydroxy-5-methylisoxazol-4-yl)propionate] and KA (kainate) receptors, named after their selective exogenous agonists (Figure 2). Among these classes, NMDA receptors

(NMDARs) and AMPA receptors (AMPA) are the most studied, particularly NMDARs,<sup>9,10</sup> while KA receptors, which are thought to be involved in the modulation of Glu and GABA release in selected brain regions, such as hippocampus, also *via* “metabotropic” mechanisms,<sup>11</sup> are much less characterized.

All ionotropic glutamate receptors exist as tetrameric complexes, whose composition, in terms of subunits, is strongly dependent on stage of development, brain region and cell type.<sup>12,13</sup> The channel pore is formed by the transmembrane domain of the four receptor subunits, while the ligand binding site is located at the extracellular domain, near the N-terminus. An intracellular C-terminus domain is also present in all subunits. In addition, NMDARs contain a co-agonist binding site, located at the extracellular domain of an obligatory NR1 subunit. This co-agonist site is continually occupied, in basal conditions, by glycine (Gly), or D-serine (D-Ser),<sup>4</sup> an unusual D-amino acid synthesized in human brain.<sup>14</sup>

AMPA and NMDARs are co-localized, at postsynaptic level, in all the CNS, where they exert excitation of the effector neuron in two different ways, with different physiological meanings. In particular, AMPARs are responsible for the fast, short lasting depolarization of the postsynaptic membrane, following Glu binding, while NMDARs are later activated, and sustain the excitation of the Glu-stimulated neuron for a longer time, resulting in the long term potentiation (LTP) of the transmission.<sup>12</sup> These differences reflect the different mechanisms of activation of these two ion channels.

Indeed, while Glu binding is sufficient to activate AMPARs, and hence to rapidly deal an excitatory input, NMDARs are considered as “coincidence

detectors”, because they are activated just when Glu binding and membrane depolarization are concomitant. In their resting state, NMDARs are blocked by extracellular  $Mg^{2+}$  ions, which impede  $Ca^{2+}$  entrance in the postsynaptic cell. Change in the membrane potential, caused by AMPARs activation, displaces  $Mg^{2+}$  from the channel pore and, in presence of Glu and Gly (or D-Ser) binding, switches the receptors into the active state, allowing  $Ca^{2+}$  intake and prolonged excitation of the cell.

### Metabotropic receptors

In addition to the prompt excitatory activity, mediated by glutamate-gated ion channels, Glu also exerts more complex actions, interacting with specific G protein coupled receptors (GPCRs). These metabotropic Glu receptors (mGluX) belong to the family C of GPCRs and, besides the classical transmembrane heptahelical structure, are characterized by the *Venus flytrap* long extracellular domain, which contains the ligand binding site.<sup>15</sup>

Different subtypes of mGluX are known, which are divided into three groups. Many subtypes are also subject to alternative splicing and present differences in the intracellular C-terminus tails:

- Group I, which includes mGlu1 and mGlu5;
- Group II, which includes mGlu2 and mGlu3;
- Group III, which includes mGlu4, mGlu6, mGlu7 and mGlu8.

As well as ionotropic glutamate receptors, mGluX are widespread in the CNS, but, in contrast, the presynaptic, or even extrasynaptic localization is a common feature of many subtypes. Group I mGluX,

mostly postsynaptic, are coupled to  $G_q$  proteins and activate phospholipase C, leading to intracellular production of inositol 1,4,5-trisphosphate ( $IP_3$ ) and diacylglycerol. The downstream signalling cascade results in the mobilization of intracellular  $Ca^{2+}$  and increase in the cellular excitability, through the positive modulation of different ion channels. Groups II and III mGluR, conversely, are often localized at presynaptic sites and couple to  $G_{i/o}$ . They are associated to modulatory actions, mainly on the release of Glu, GABA and other neurotransmitters, exerted *via* the inhibition of adenylate cyclase.

## 2.2. Clinical relevance of glutamatergic system

It is not surprising that all the vital physiological functions which Glu is responsible for have switched on a great interest about the chance to interfere with the glutamatergic system, in order to face complex clinical challenges, particularly in the field of CNS diseases. Although the large volume of preclinical and clinical studies performed and on-going, only the dissociative anaesthetic ketamine and memantine, the first approved glutamatergic drug for Alzheimer's disease, have found clinical use (Figure 3, **1** and **2**).<sup>4</sup> These two drugs share the same pharmacological action, that is the block of NMDARs mediated neuron excitability. Indeed, ketamine is a non-competitive NMDARs antagonist, inhibiting the receptor activity by binding to the phencyclidine allosteric site,<sup>16</sup> while memantine is considered an uncompetitive, voltage-dependent NMDARs antagonist, mimicking the modulatory function of  $Mg^{2+}$  on the ion channel gating.<sup>17</sup>

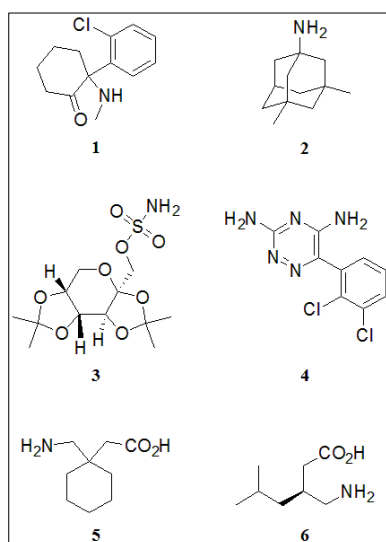


**Figure 3.** Drugs modulating the glutamatergic transmission in clinical use.

However, the anti-glutamatergic activities found in antiepileptic drugs, designed as sodium channels blockers, such as topiramate (**3**) and lamotrigine (**4**), or as GABA-ergic agents, such as gabapentin (**5**) and pregabalin (**6**),<sup>18</sup> sustain the therapeutic usefulness of modulators of the glutamatergic transmission.

Since the very early evidences of the involvement of Glu in the generation of

excitotoxic injury<sup>19</sup> and in inducing seizures,<sup>20</sup> research on glutamatergic agents for therapy was driven towards the modulation of the fast, excitatory effects of ionotropic receptors, in particular clinical states, such as trauma, ischemia and epilepsy. Particularly in trauma and cerebral stroke, the challenge to block the secondary brain damage, often as lethal as the primary insult, sustained by NMDARs mediated transmission, but emerging in a delayed time with respect to the deleterious event, has been an attracting issue for decades. However, due to the number of side effects of known NMDARs antagonists, their clinical use is very limited and subject of discussions.

On the other hand, a relatively recent switch towards the regulation of metabotropic glutamate receptors, potentially useful to treat more complex chronic neurodegenerative and psychiatric conditions, such as Alzheimer's disease, Parkinson's disease, schizophrenia, depression, amyotrophic lateral sclerosis, multiple sclerosis and so on, is noticeable.

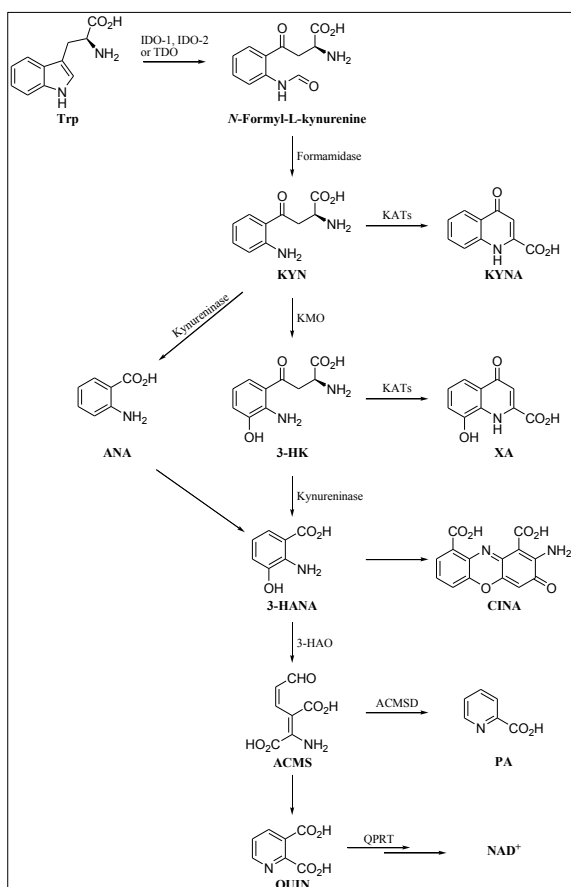
All drugs in clinical studies can be considered as "direct" modulators of the glutamatergic transmission, as well as they target molecular components directly involved in the Glu pharmacology. Thus, subtype specific antagonists of ionotropic receptors and Group I metabotropic receptors, as well as Group II and III metabotropic receptors agonists are under study, together with examples of both positive and negative allosteric modulators of virtually all glutamate receptors, and with some drugs targeting Glu transporters.<sup>4</sup> Here I propose a different way to face the challenge: instead of directly targeting the glutamatergic transmission, interfering with metabolic pathways, which have been demonstrated to produce metabolites able to somehow interact with the glutamatergic system, could be a viable alternative to finely modulate Glu effects,

avoiding the well-known CNS side effects of traditional glutamatergic drugs.

This is the case of the kynurenine pathway of tryptophan catabolism which, as it will be illustrated in detail in the next pages, produces a number of neuroactive metabolites, whose interactions with the glutamate system are nowadays a consolidated feature.

## Section 3. KYNURENINE PATHWAY

### 3.1. Overview



**Scheme 1.** Kynurenine pathway of tryptophan metabolism.

L-Tryptophan (Trp) is an essential, proteinogenic amino acid and, in humans, it is also the biological precursor of two compounds extremely important for a lot of vital physiological processes, namely the neurotransmitter serotonin and the hormone melatonin. However, most of the Trp introduced with the diet is processed by a different pathway, which is commonly known as the “kynurenine pathway” (KP,

Scheme 1) of tryptophan degradation.<sup>21–25</sup> In this

section the KP will be described in detail, focusing on the specific activities of KP metabolites in the CNS and on the diseases that have been related to dysregulations of the pathway, in which a fine tuning of this complex enzymatic cascade is proposed to be an useful point of intervention for drug discovery.



This ubiquitous enzymatic route (principal sites of localization are the liver and the macrophages in periphery, with regulatory roles upon the immune system, and microglia and astrocytes in the CNS, while KP is almost, but not totally,<sup>26</sup> absent in neurons) is responsible for more than 90% of Trp catabolism<sup>27</sup> and for the production of the cofactor NAD<sup>+</sup>, which is crucial for the performing of redox reactions at both cellular and mitochondrial levels.

The first, rate limiting step of the KP is the oxidative ring opening of Trp, catalysed by indoleamine 2,3-dioxygenase (IDO), of which two isoforms are known, IDO-1<sup>28</sup> and IDO-2.<sup>29</sup> In the liver, this transformation is performed by tryptophan 2,3-dioxygenase (TDO), a more substrate specific, heme-dependent enzyme.<sup>30</sup> The product of this reaction, *N*-formyl-L-kynurenine, is then converted into L-kynurenine (KYN) by formamidase.

Enzymes responsible for these two biosynthetic steps are much less active in the brain than in periphery,<sup>31</sup> but KYN is able to reach the CNS through specific transporters.<sup>32</sup> For this reason, the true first event of the KP in the brain is considered to be the blood-derived income of this metabolite.

KYN, which the entire pathway is named from, is the key intermediate, because it gives origin to the two branches of the KP, whose downstream metabolites are able to influence excitatory amino acids neurotransmission. Interestingly, these two arms are physically separate in the CNS and are prerogative of non-neuronal cells.<sup>33</sup> Kynurenine aminotransferase II<sup>34</sup> (KAT II, one of the four KATs characterized in humans)<sup>35</sup> is the enzyme responsible, in the brain, for the specific,

irreversible transamination of KYN, yielding kynurenic acid (KYNA), which is a dead-end product, endowed with neuroprotective activities, of the pathway. This transformation occurs in astrocytes.<sup>33</sup>

On the other hand, microglial cells utilize a different enzymatic pool to process KYN and some of the metabolites belonging to this branch of the KP can act, in pathological conditions, as neurotoxins. This potentially neurotoxic cascade starts with the actions of kynurenine 3-monooxygenase (KMO) and kynureninase, which are responsible for the conversion of KYN into 3-hydroxykynurenine (3-HK) and anthranilic acid (ANA), respectively.<sup>36</sup>

3-HK, as well as KYN, is the substrate of competing enzymes: KATs, which synthesize xanthurenic acid (XA),<sup>37</sup> and kynureninase, which degrades 3-HK to 3-hydroxyanthranilic acid (3-HANA).<sup>38</sup> The latter is preferably obtained in the brain, for unknown reasons, from ANA.<sup>39</sup>

3-HANA, in a minor extent, auto-oxidizes and dimerizes to form cinnabarinic acid (CINA),<sup>40</sup> but for the most is converted by 3-hydroxyanthranilic acid 3,4-dioxygenase (3-HAO)<sup>41</sup> into 2-amino-3-carboxymuconic-6-semialdehyde (ACMS) which, in physiological conditions, spontaneously rearranges to form quinolinic acid (QUIN). 2-Amino-3-carboxymuconic-6-semialdehyde decarboxylase (ACMSD)<sup>42</sup> is responsible for the peripheral conversion, under non-physiological conditions, of ACMS into picolinic acid (PA).

Finally, QUIN is the substrate of quinolinate phosphoribosyltransferase (QPRT), responsible for the first step of the transformation of QUIN into  $\text{NAD}^+$ . The activity of this enzyme, a gatekeeper for the synthesis of

$\text{NAD}^+$ , is very low in the brain, compared to that of 3-HAO, and basal QUIN concentrations are 40-60 times higher than those of 3-HANA.<sup>43</sup>

### 3.2. Neuroactive kynurenines

Since the observation that several “kynurenines”, a term commonly used to indicate all KP metabolites, are endowed with specific biological activities, the KP is attracting more and more interest and its modulation is nowadays considered a promising target for the development of novel therapeutic approaches, in particular in the field of CNS disorders.<sup>23</sup> Indeed, modifications in the balance between neuroprotective and neurotoxic kynurenines have been observed in several CNS pathological conditions.<sup>24</sup>

Proceeding in the direction of the cascade, from Trp, the first neuroactive metabolite encountered is KYNA.

KYNA, produced in and released by astrocytes, is present in human brain in exceptionally high levels,<sup>44</sup> compared to other mammals. This is reasonably related to the peculiar neurological activities of KYNA.

In particular, KYNA is universally considered an endogenous neuroprotective agent, mostly for its ability to block, in a competitive fashion, all excitatory ionotropic glutamate receptors,<sup>45</sup> with high affinity for the glycine co-agonist site of NMDARs,<sup>46</sup> antagonizing the Glu-induced excitotoxicity. Additionally, the neuroprotective action of KYNA is also attributable to non-receptors mediated activities, as antioxidant and free radicals scavenger, intrinsic properties related to its chemical structure.<sup>47</sup>

Recently, KYNA has been discovered to also play a role in cholinergic transmission in the CNS, acting as a negative allosteric modulator of  $\alpha 7$  nicotinic acetylcholine receptors ( $\alpha 7$ nAChRs).<sup>48</sup> Its inhibitory activity

towards presynaptic  $\alpha 7$ nAChRs results in reduced Glu release and decreased glutamatergic and cholinergic transmissions.<sup>49</sup>

Regarding the microglial branch of the KP, known neuroactive metabolites include:

- 3-HK, whose deleterious actions in the CNS are mainly explicated by its tendency to auto-oxidize and form neurotoxic free radical species;<sup>50</sup>
- XA, a recently discovered potential endogenous modulator of Group II metabotropic Glu receptors (mGlu2 and mGlu3);<sup>37</sup>
- CINA, the product of auto-oxidation and dimerization of 3-HANA, which acts as a selective orthosteric partial agonist of mGlu4, responsible for neuroprotective effects;<sup>40</sup>
- QUIN, selective NMDARs agonist, able to induce excitotoxic stress in pathological conditions.<sup>51</sup>

Among all these neuroactive KP metabolites, the most investigated and characterized one is certainly QUIN. Neuroscientists' interest for this endogenous toxin dates back to the first observation that intracerebroventricular injection of QUIN causes seizures in treated mice.<sup>52</sup> This fits with the ability of QUIN to selectively activate NMDARs, with higher potency in the forebrain,<sup>53</sup> and to induce abnormal neuronal excitability.

In addition, localized QUIN administration in selected brain regions is nowadays an exploited model of neurodegeneration, useful to study the biomolecular framework of CNS diseases at the early stages of progression.<sup>54–56</sup>

### 3.3. Kynurenine pathway related pathologies

Several experimental observations along the past 25 years have found relationships between impairment of the correct homeostasis of kynurenines metabolism and a wide number of often highly invalidant neuropathological conditions, including both neurodegenerative diseases and psychiatric disorders, such as depression and schizophrenia.<sup>24</sup>

Neurological pathologies that have been linked to the KP include epilepsy,<sup>57</sup> Alzheimer's disease,<sup>58</sup> Parkinson's disease,<sup>59</sup> AIDS-related dementia,<sup>60</sup> amyotrophic lateral sclerosis,<sup>61</sup> multiple sclerosis (MS)<sup>62</sup> and Huntington's disease (HD).<sup>63</sup> Since a complete dissertation about all KP related pathologies overcomes the aim of this PhD thesis work, only the implications of altered kynurenines pattern in two specific diseases, namely HD and MS, will be described here.

#### Huntington's disease

HD<sup>64</sup> is an inherited, genetic disease caused by mutation of a single gene, encoding for the ubiquitous protein huntingtin, whose physiological function is still unknown. The presence of the mutated protein produces precipitation of inclusion bodies in neurons and increases the rate of neuronal death, primarily in the cortex and in the striatum.

These damages result in the development of characteristic symptoms: cognitive deficiency, uncontrollable movements (“*chorea*”) and also psychiatric disorders, such as anxiety and depression, are common features in HD patients.

To date, no effective therapies are available for this invalidant condition, which is only treated with agents useful to relieve symptoms, especially kinetic and psychiatric symptoms.

Most of efforts sustained in HD research are now aimed at the complete comprehension of the roles of the KP in the early stages of the disease and at validating the manipulation of the Trp metabolism as a preferred target for future drug discovery in this field.

Indeed, a lot of consistent experimental evidences sustains the “kynurenergic hypothesis” of HD, at least for what is concerning the onset and the early stage progression of clinical manifestations:

- activation of the microglial branch of the KP was found in early grade HD patients;<sup>65</sup>
- high cortical and neostriatal levels of QUIN emerged from *post mortem* data;<sup>66</sup>
- increase in neurotoxic 3-HK and QUIN levels in transgenic mouse models of the disease are mostly recordable in the cortex, striatum and cerebellum, that are the most damaged brain tissues in HD patients;<sup>67</sup>
- KMO and 3-HAO genes deletion partially abolishes mutated huntingtin toxicity in yeast models of HD;<sup>63</sup>
- KATs genes deletion, again in yeasts, exasperates mutated huntingtin toxicity, by blocking the biosynthesis of neuroprotective KYNA.<sup>63</sup>

All this indications attribute to the over-activation, in HD patients, of the microglial branch of the KP, and to the consequent increased

QUIN/KYNA ratio, a crucial pathogenic role in the development and the propagation of neuronal mortality, especially in those brain regions that suffer the most damage.<sup>66</sup> Therefore, modulation of KP enzymes, in particular those responsible for the production of neurotoxic metabolites, such as KMO and 3-HAO, is today a key topic in the set-up of novel therapeutic approaches to the treatment of HD.

### Multiple sclerosis

Unlike for HD, the possible relationship between the KP and MS is a relatively new and contradictory topic. Nevertheless, the consolidated role of the KP in the control of both immune system and brain functions,<sup>68</sup> the two main actors in an autoimmune neurodegenerative disease, such as MS is, makes this a field of increasing interest for neuroscientists. In addition, recent observations of modified KP profiles in MS patients and animal models suggest the involvement of Trp metabolism in some MS pathological events.<sup>62</sup>

What is still unclear is at what level of the KP and at what stage of disease evolution, pharmacological intervention could be useful.

Once more, the ability of kynurenines to interfere with the Glu mediated excitatory transmission may be an indication of a connection between altered KP profile and MS, together with the following experimental evidences:

- MS patients have low Trp concentrations in serum and cerebrospinal fluid, suggesting activation of the KP;<sup>69</sup>



- KYNA levels are increased during the active phase of MS,<sup>70</sup> while patients in the chronic, inactive phase, present low KYNA levels;<sup>71</sup>
- one of the hallmarks of MS lesions is the presence of activated microglia and perivascular macrophages along the boundary of the lesion site.<sup>72</sup> These activated cells may be responsible for QUIN production in concentrations sufficient to induce death of both neurons<sup>73</sup> and oligodendrocytes;<sup>74</sup>
- IDO-1 inhibition by 1-methyl-L-tryptophan exacerbates the disease status in experimental autoimmune encephalomyelitis (EAE) animal models;<sup>75</sup>
- QUIN and 3-HK, synergistic neurotoxic kynurenines, have been found at high levels in the spinal cord of EAE rats.<sup>76,77</sup>

Although the role of Trp metabolites in MS is far from being completely understood, several indications drive the scientists to keep on the investigation in this field, which appears an attracting starting point for the development of new “kynurenergic” treatments for patients affected by MS. The most promising approach, as well as in HD research, seems to be the switch of the balance between the two branches of KYN metabolism in favour of the production of KYNA, by blocking the activity of enzymes like KMO and 3-HAO, responsible for the synthesis of neurotoxic metabolites, 3-HK and QUIN, respectively.

#### Section 4. AIM OF THE WORK

The aim of the present work was to identify novel, chemically stable compounds endowed with inhibitory activity towards 3-HAO, the KP enzyme responsible for the synthesis of QUIN. Pyridine *N*-oxide was chosen as a suitable scaffold for the design of potential 3-HAO inhibitors.

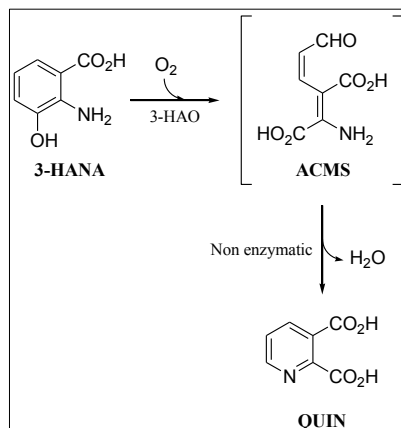
Objective of this study was as well the evaluation of the beneficial effects of decrease in QUIN levels, caused by 3-HAO inhibitors synthesized in this work, in contrasting NMDARs mediated neurotoxicity in models of both HD and MS.

3-HAO inhibition tests, both *in vitro* and *in vivo*, were performed at the Maryland Psychiatric Research Center - University of Maryland - Catonsville, by Prof. Schwarcz's research group. For MS related study, EAE mice were treated with the most active compound described here, at the Istituto Neurologico Mediterraneo - Neuromed - Pozzilli, in collaboration with Prof. Nicoletti's research group.

In order to allow readers to understand the rationale that sustained this PhD project, this section is dedicated to the description of the target enzyme, 3-HAO, focusing on its biochemical features, known inhibitors and implications in CNS diseases.

#### 4.1. 3-Hydroxyanthranilic acid 3,4-dioxygenase

QUIN, the precursor of the pyridine core of nicotinamide cofactors, but also a known endogenous neurotoxin acting *via* activation of glutamatergic transmission, is synthesized, in the CNS, by microglial 3-HAO.<sup>41</sup>



Human 3-HAO is a 286 amino acids

protein, belonging to the family of extradiol dioxygenases. Like in other congeners, a non-heme Fe(II) ion serves as the cofactor for the catalysis. The reaction between 3-HAO and substrate results in the net addition of molecular oxygen to 3-HANA, causing aromatic ring opening at positions C<sub>3</sub>-C<sub>4</sub>. Spontaneous loss of water in the highly unstable intermediate ACMS leads to the production of QUIN (Scheme 2).

Human 3-HAO is largely expressed in peripheral tissues, mainly in liver and macrophages, but it is also present in the CNS. This enzyme is widespread in eukaryotes, but the recent identification of the biosynthesis of QUIN from Trp in bacteria<sup>78</sup> made possible a good characterization of its structural and functional features, *via* the analysis of crystal 3-HAO in the unliganded form, in complex with the natural substrate and in complex with the well-known 3-HAO inhibitor, 4-chloro-3-hydroxyanthranilic acid (4-Cl-3-HANA),<sup>79</sup> from *Ralstonia metallidurans*.<sup>80</sup>

Crystal structure of the human functional enzyme is not so far available, due to the instability of the purified protein. Nevertheless, a monophosphate structure, in which the catalytic Fe(II) ion is replaced by Ni(II) due to the purification protocol, was resolved by Bitto *et al.* in 2007, and deposited in the Protein Data Bank (PDB ID: 2QNK, <http://www.rcsb.org>).

In addition, crystal structure of 3-HAO from bovine kidney, which shares 86.7% identity with the human protein, was recently published.<sup>81</sup>

Enzymes from *Ralstonia metallidurans*, and from other bacteria and simple eukaryotes, e. g. yeast *Saccharomyces cerevisiae*<sup>82</sup>, present shorter

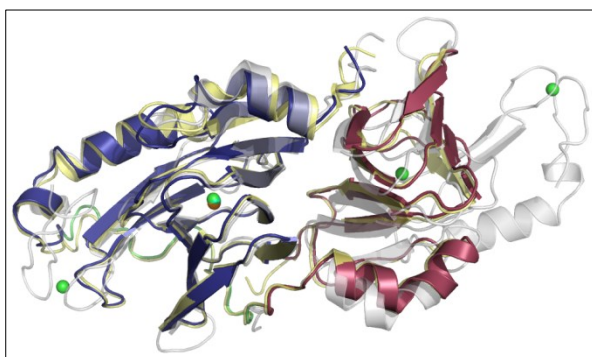


**Figure 4.** Cartoon showing the superposition of 3-HAO crystal structures from *Saccharomyces cerevisiae* (ID 1ZVF; homodimer; grey, complexed nickel ions in green), *Homo sapiens* (ID 2QNK; monomer; yellow, complexed nickel ion in green) and *Bos taurus* (ID 3FES; monomer; domain A in blue, domain B in red, linking domain in green and complexed iron ion in orange).

chains, 174 and 176 residues, respectively, and operate as homodimers.<sup>80</sup> Conversely, mammalian 3-HAO is a monomer, divided in two distinct

domains, linked by a long stretch (residues 161-177): domain A (residues 1-160), containing the

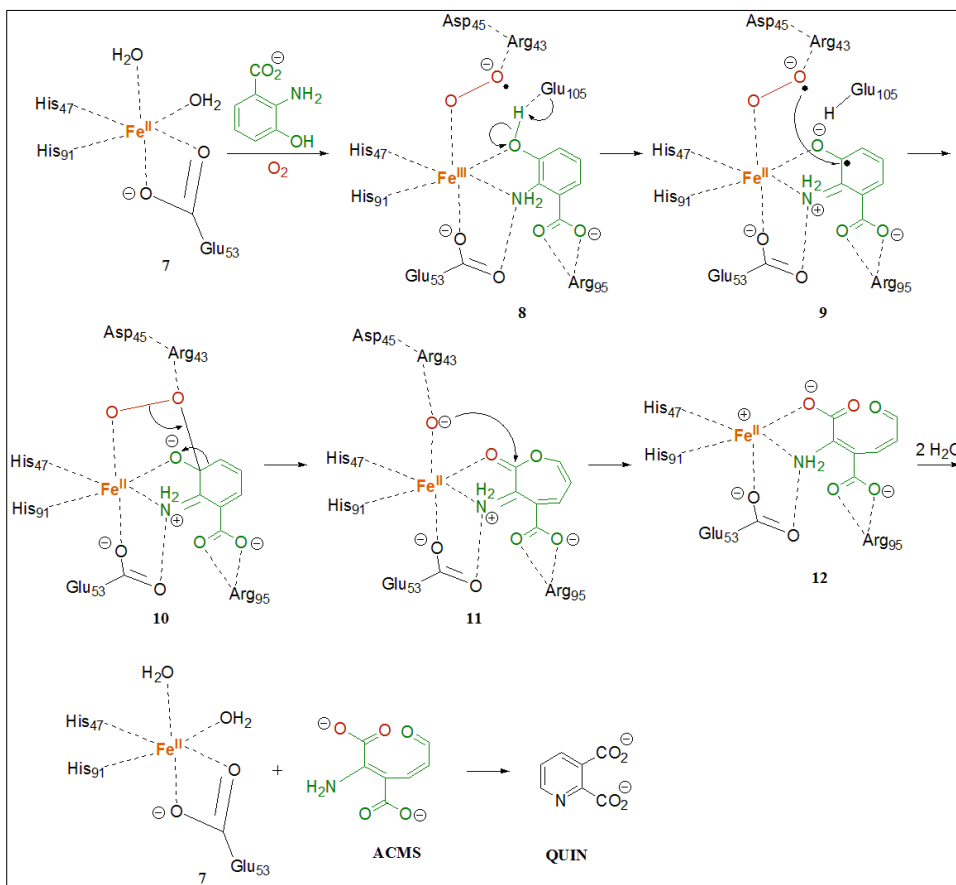
active site, superposes quite well with the monomer of yeast 3-HAO; domain B (residues 178-286), smaller, superposes with part of the second monomer in the homodimeric yeast complex, and it is supposed to have structural role (Figure 4).<sup>81</sup>

The  $\beta$ -barrel fold, characteristic of the “cupins” family,<sup>83</sup> is the core motif of both domains A and B in the mammalian enzyme. The catalytic site is located deep inside the  $\beta$ -barrel, close to the N-terminus (domain A) and contains the fully conserved critical residues for the coordination of the metal ion. Completely conserved among the species are also most of the other residues limiting the active site cavity, in particular Arg95 and Glu105, crucial for the binding of both substrate and inhibitors, and Arg43 and Asp45, involved in the O<sub>2</sub> binding. The Fe(II) cofactor, in the bovine crystal, is five-coordinated by two residues of histidine (His47 and His91), one of glutamate (Glu53, bidentate ligand) and a water molecule.<sup>81</sup> This is in slight contrast with data from bacterial, yeast and human crystals, in which an octahedral geometry for the metal coordination site has been observed (two monodentate histidine residues, a bidentate glutamate residue and two water molecules). A second metal-binding centre is present in bacterial and yeast 3-HAO, but not in the mammalian enzyme, at the C-terminus, in which Fe(II) is coordinated by four cysteine residues. The function of this second metal site is unknown.

The complex mechanism proposed for 3-HAO catalysis, based on previous studies on catechol dioxygenases,<sup>84</sup> is depicted in Scheme 3.

The binding of the substrate to the catalytic iron ion displaces one water molecule and one coordinating oxygen atom of Glu53. Molecular oxygen then adds to Fe(II), displacing the other water molecule. Single electron transfer from Fe(II) to O<sub>2</sub> produces superoxide radical **8**, then electron-rich substrate *o*-aminophenol donates an electron to Fe(III), restoring its starting oxidation state and forming the di-radical complex **9**. Reaction between the two radical centres, followed by Criegee rearrangement,

yields seven membered lactone **11**. Hydrolysis of **11** gives ACMS, which dissociates from the enzyme and rearranges to QUIN.<sup>80</sup>



**Scheme 3.** Proposed 3-HAO catalytic mechanism.

## 4.2. State of the art of 3-HAO inhibitors

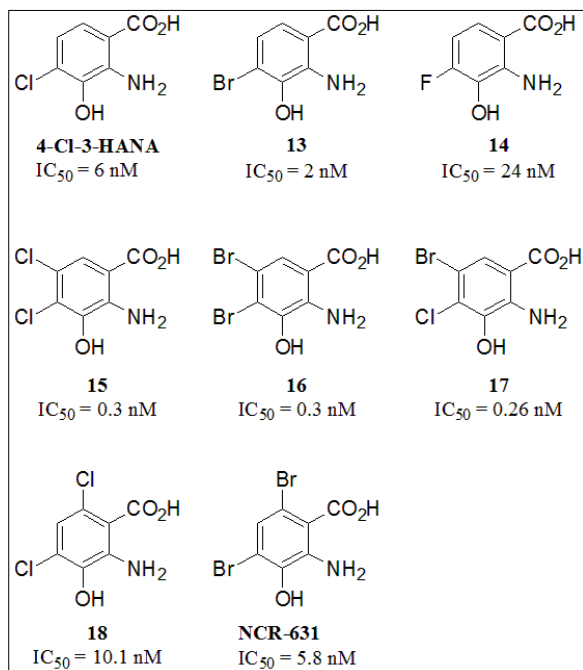


**Figure 5.** Structures of selected classic 3-HAO inhibitors and their respective  $IC_{50}$  values.

Along the past 35 years, only one class of 3-HAO inhibitors has been reported. All compounds belonging to this class share a common chemical feature: they are halogenated substrate analogues. 4-Cl-3-HANA<sup>85</sup> was the first compound able to inhibit 3-HAO identified, followed by 4-F and 4-Br derivatives.<sup>86</sup> A wider

QSAR study discovered several 4,5- and 4,6-dihalogenated 3-HANA analogues endowed with anti 3-HAO activity at low nanomolar and sub-nanomolar concentrations (Figure 5).<sup>87</sup> Despite the high activity of these inhibitors, their pharmacological and therapeutic usefulness is limited, because of the intrinsic chemical instability of this class of compounds, due to the propensity for auto-oxidation and decomposition of the *o*-aminophenol core. Indeed, with few exceptions, HPLC/UV profile after 24 hours incubation in physiological conditions showed less than 40% persistence of the inhibitors.<sup>87</sup>

However, a lot of evidences sustain the development of novel 3-HAO inhibitors as valuable tools to elucidate the role of the biosynthesis of QUIN in a wide number of pathological conditions, mainly CNS diseases:

- after spinal cord injury, systemic administration of 4-Cl-3-HANA preserves white matter survival, reduces the accumulation of QUIN at the lesion site and attenuates secondary functional deficits in guinea pigs, without increasing KYNA levels;<sup>88</sup>
- 4,6-dibromo-3-hydroxyanthranilic acid (NCR-631) attenuates anoxia-induced neuronal loss and completely abolishes lipopolysaccharide (LPS)-induced neurotoxicity *in vitro*;<sup>89</sup>
- NCR-631 provides increase in the latency time and reduction in the severity of seizures induced by both pentylenetetrazole treatment in rats and proconvulsant sound exposure in mice;<sup>90</sup>
- NCR-631 is effectively absorbed after intragastric administration and induces a dose dependent 3-HANA accumulation both in serum and in the brain. However, the effect is limited in time, because of both chemical and metabolic instability (high-rate liver metabolism).<sup>91</sup>



### 4.3. Design of novel pyridine *N*-oxide based 3-HAO inhibitors

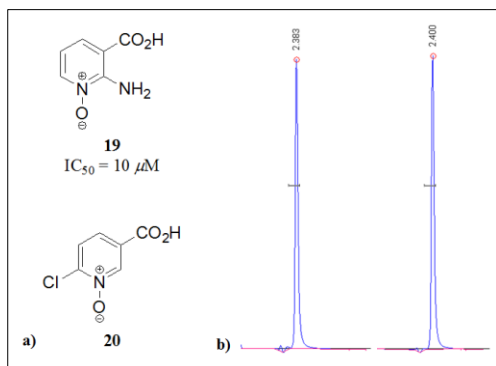


**Figure 6.** a) Structures of 2-aminonicotinic acid 1-oxide, the first non 3-HANA derived 3-HAO inhibitor (**19**) and inactive analogue 6-chloronicotinic acid 1-oxide (**20**). b) Chromatograms at T = 0 (left) and T = 24 hours (right) registered during **19** stability test, showing complete chemical stability.

needed for the binding of the catalytic Fe(II) and for the correct positioning into the active site, as well as the electronic properties of the speculated enzyme-substrate transition state (Figure 7).<sup>80</sup> 2-Aminonicotinic acid 1-oxide fits quite well these requirements, as carboxylic group should provide binding to Arg95, 2-amino-1-oxide functionality superposes

to *o*-aminophenol core of both substrate and reported inhibitors, and pyridine nitrogen shares with carbon C<sub>3</sub> of 3-HANA the same poor electron density. In addition, compound **19** could be seen as a resonance hybrid, with one iminium ion containing contributing

During my Laurea thesis work, I have described the first, chemically stable 3-HAO inhibitor not bearing the *o*-aminophenol core, 2-aminonicotinic acid 1-oxide (Figure 6, **19**), based on the pyridine *N*-oxide scaffold. This structure was selected in order to mimic the structural features

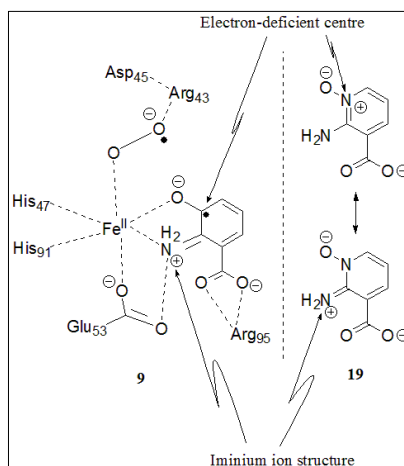


**Figure 7.** Structural and electronic analogies between **19** (right) and 3-HAO/3-HANA complex **9** in the proposed transition state of the catalysis (left).

structure, similar to that proposed as one of the transition states of 3-HAO catalysis.

The above mentioned work, in addition to confirm the suitability of pyridine *N*-oxide for the design of novel 3-HAO inhibitors, also suggested that amino group at position C<sub>2</sub> of the pyridine ring is essential for activity, since 4-chloronicotinic acid 1-oxide (Figure 6, **20**) resulted completely inactive.

With these data in hands, in order to find novel 3-HAO inhibitors and to define a preliminary SAR profile, several compounds were synthesized, making modifications to the base structure of compound **19**. 2-Amino group was maintained in all the synthesized compounds, while the essentiality of the *N*-oxide group, replacement of the carboxylate at position C<sub>3</sub> and introduction of substituents, diverse in structural and electronic properties, were individually investigated.

## Section 5. RESULTS AND DISCUSSION

### 5.1. *In vitro* 3-HAO inhibition

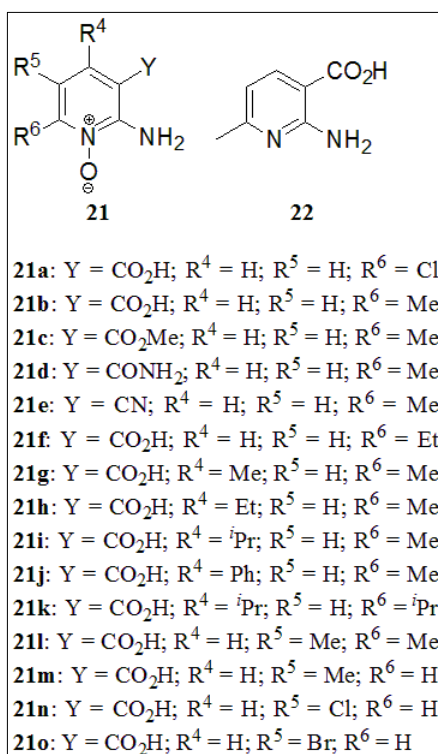


**Figure 8.** Structures of all the compounds synthesized in this work.

All the compounds designed as 3-HAO inhibitors (Figure 8) were tested *in vitro* both in rat and human brain homogenate, investigating the decrease in the production of QUIN, by quantitative analysis of radiolabelled <sup>13</sup>C-QUIN after incubation of the samples with <sup>13</sup>C-3-HANA and test compounds.

The exploration of the 2-aminopyridine 1-oxide nucleus of novel 3-HAO inhibitors started with the insertion of a Cl substituent at position C<sub>6</sub>. This modification, which led to the synthesis of compound

**21a**, was chosen for structural analogy with 4-Cl-3-HANA. Activity *in vitro* was confirmed for this compound, although a slight decrease in 3-HAO % inhibition at 10 μM was observed, with respect to compound **19**, in human brain homogenate (57.0% vs 65.8% inhibition).

Replacement of the Cl substituent with a methyl group gave compound **21b** and allowed the evaluation of the electronic properties of C<sub>6</sub> substituents, in terms of their effect on 3-HAO inhibitory activity. Indeed,

the observation of the high activity which 6-methyl substituted **21b** is endowed with ( $IC_{50} = 0.6 \mu M$ ) suggests that electron-donating groups are preferred, in order to increase the potency of 2-aminopyridine 1-oxide derivatives as 3-HAO inhibitors.

At this stage the confirmation of the relevance of the *N*-oxide motif for the activity came from compound **22**, which bears all the structural features of the most potent molecule of this series, **21b**, except for the oxidized pyridine nitrogen. **22** resulted completely inactive, validating the need of *N*-oxide mediated coordination of the catalytic Fe(II) of 3-HAO.

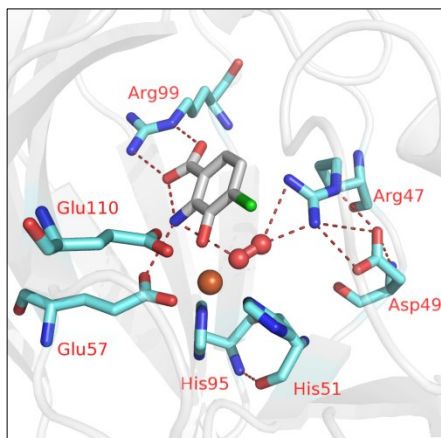


**Figure 9.** Snapshot of the active site of 3-HAO/4-Cl-3-HANA/O<sub>2</sub> complex (PDB ID 1YFW) from *Ralstonia metallidurans*, showing interactions between inhibitor and crucial enzyme residues.

In order to equip novel 3-HAO inhibitors with better physical-chemical properties, compatible with brain penetration after systemic administration, three compounds, in which the C<sub>3</sub> carboxylate of **21b** was replaced with, respectively, its methyl ester, a carboxamide and a cyano group (compounds **21c-e**) were synthesized and tested. None of these derivatives presented significant activity. Though **21e** inactivity was predictable, based on the supposed bidentate arginine trapping in which 4-Cl-3-HANA is involved in the enzyme/inhibitor complex from *Ralstonia metallidurans* (Figure 9),<sup>80</sup> inactivity of **21c** and, especially, **21d** was not so expected. These data suggest that a function bearing a net negative charge at physiological pH, like most of carboxylic acids do, is essential to take bond with Arg95

(mammalian enzyme, Arg99 in 3-HAO from *Ralstonia metallidurans*), for the correct positioning of the inhibitor in the active site.

Thus, once learned that 1-oxide and 2-amino groups, together with C<sub>3</sub> free carboxylate, are irreplaceable functionalities, the further exploration was aimed at evaluating the possibility to introduce different substituents at positions C<sub>4</sub>, C<sub>5</sub> and C<sub>6</sub>, and their effect on activity.

The first change to the structure of **21b** applied was the one carbon elongation of the methyl group at position C<sub>6</sub>, replacing it with an ethyl. Compound **21f** showed significant inhibition only at high concentrations (1 mM).

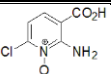
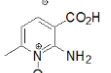
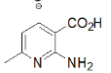
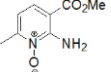
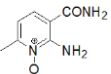
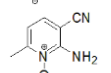
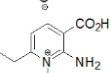
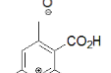
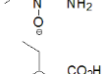
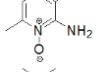
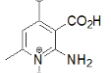
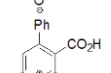
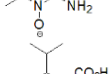
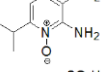
The screening then proceeded *via* the application, one by one, of the following modifications:

- introduction of methyl, ethyl, isopropyl and phenyl groups at position C<sub>4</sub>, maintaining C<sub>6</sub> methyl (**21g-j**; **21k**, di-isopropyl substituted at C<sub>4</sub> and C<sub>6</sub>, was chosen due to synthetic accessibility);
- introduction of methyl group at position C<sub>5</sub>, maintaining C<sub>6</sub> methyl (**21l**);
- elimination of C<sub>6</sub> methyl, and introduction of both methyl (electron-donating) and halogen (electron-withdrawing) substituents at position C<sub>5</sub> (**21m-o**).

Among structures **21g-m**, only **21l** showed interesting activity: although it is less potent than other active analogues, its IC<sub>50</sub> value is less than 100  $\mu$ M in human brain homogenate, while **21m** is responsible for only slight

inhibition at the same concentrations. Data from tests on **21n** and **21o** are still not available.

All the biological results are summarized in Table 1.

Compound	Rat 3-HAO % inhibition			Human 3-HAO % inhibition		
	10 $\mu$ M	100 $\mu$ M	1 mM	10 $\mu$ M	100 $\mu$ M	1 mM
	48.6	79.0	100.0	57.0	93.6	100.0
	89.5	100.0	100.0	91.8	97.2	100.0
	-	-	32.3	-	-	27.6
	-	-	9.3	-	-	9.5
	2.7	-3.5	9.3	2.7	2.3	19.8
	-	-	-6.3	-	-	6.3
	-	-	90.9	-	-	89.0
	-	-	38.0	-	-	68.2
	-5	-1	-	N/A <sup>a)</sup>		
	-	-3	-	N/A <sup>a)</sup>		
	7.3	21.4	87.5	4.5	15.8	68.1
	3.0	11.2	71.2	7.4	11.7	57.4
	-	40.6	79.5	-	67.8	81.3
	-	31.1	69.5	-	16.4	57.4

**Table 1.** Summary of the 3-HAO inhibitory activity of all the synthesized compounds. Biological tests were performed in both rat and human brain homogenate, measuring the production of <sup>13</sup>C-QUIN after incubation with <sup>13</sup>C-3-HANA and different concentrations of test compounds. Activities are expressed as percentage of inhibition of 3-HAO. Colours: cyan, most active compound; green, less active but still interesting compounds; orange, compounds active only at high concentrations; grey, completely inactive compounds. *a)* Tested in rat liver homogenate.

## 5.2. SAR

Results from biological tests discussed in the previous paragraph, combined with data deriving from the docking of **21b** in the active site of human 3-HAO performed by our group of computational chemistry, allowed to define a preliminary SAR profile for this class of molecules, with respect to the ability to inhibit 3-HAO (refer to Figure 10).

- 1) Pyridine *N*-oxide is a suitable core for the design of 3-HAO inhibitors.
- 2) 2-Amino group, as well as 1-oxide, is essential for activity.
- 3) Y substituent must contain a negatively charged function at physiological pH, and the one which has been identified in this work is carboxylate.

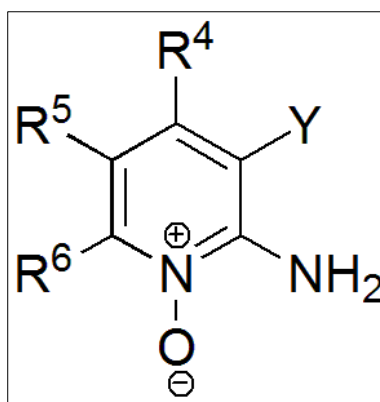


**Figure 10.** Base scaffold of novel 3-HAO inhibitors designed in this work.

- 4) Activity is increased by electron-donating substituents, while it is decreased by electron-withdrawing groups, with respect to R<sup>6</sup>.
- 5) Elongation of R<sup>6</sup> leads to loss of activity.
- 6) Hydrocarbon substituents at position C<sub>4</sub> are not tolerated.
- 7) R<sup>5</sup> = Me reduces activity.



### 5.3. *In vivo* tests

Compound **21b** was assayed for its ability to decrease QUIN levels in lesioned rat brain, *in vivo*.

Brain injury was induced by QUIN injection in the striatum. After one

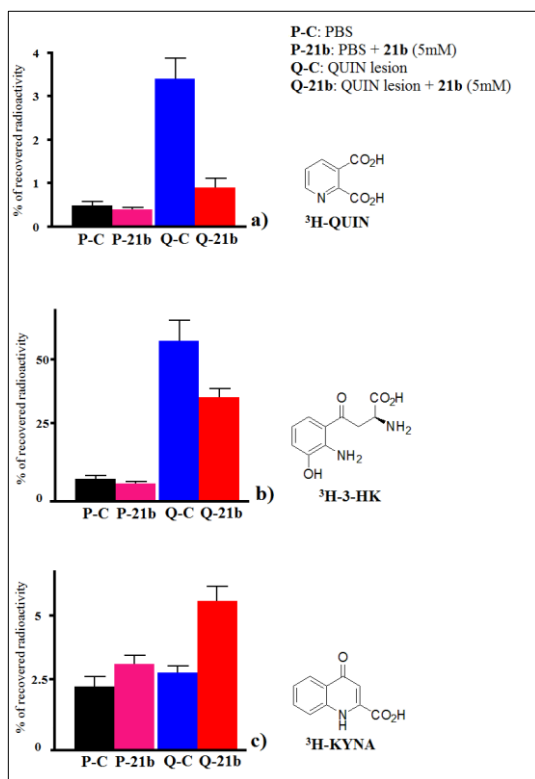


**Figure 11.** Plots resuming results of **21b** *in vivo* 3-HAO inhibition test.

Black bars refer to non **21b**-treated healthy brains (control); pink bars refer to **21b**-treated healthy brains; blue bars refer to non **21b**-treated lesioned brains; orange bars refer to **21b**-treated lesioned brains.

**a)** Detected tritiated QUIN levels. **b)** Detected tritiated 3-HK levels. **c)** Detected tritiated KYNA levels.

PBS: phosphate buffered saline.

week, animals were treated by intrastriatal administration of  $^3\text{H}$ -KYN, followed by **21b**. Quantitative analysis of  $^3\text{H}$ -QUIN,  $^3\text{H}$ -3-HK and  $^3\text{H}$ -KYNA on both lesioned and control tissues showed that **21b** is able to substantially decrease the production of QUIN in unfunctional brain *in vivo*. An effect on both 3-HK and KYNA levels was as well observed: 3-HK production decreased, while KYNA concentration increased in injured brain, after **21b** treatment. (Figure 11)

These findings confirm that 3-HAO inhibitor **21b** interferes

with the KP, and therefore with the excitatory glutamatergic transmission, switching the balance between neurotoxic (QUIN, 3-HK) and

neuroprotective (KYNA) metabolites towards the latter, in an *in vivo* animal model of neurodegenerative condition.

Further, **21b** could be a valuable tool to study, in more complex models, the possibility to interfere with neurodegeneration mechanisms in chronic CNS diseases, in which involvement of Trp metabolism has been proposed.

Accordingly, **21b** was assayed in EAE mice, animal model of MS, showing interesting preliminary results. This test was aimed at the evaluation of changes in the concentrations of KP metabolites, in particular CINA, in different tissues, secondary to 3-HAO inhibition, in mice previously immunized *via* systemic administration of LPS. Since systemic LPS induces KP enzymes expression, even in the CNS,<sup>92</sup> changes in Trp metabolites profile are expected to be related to brain functional loss, typical of immune-based neurodegenerative diseases, such as MS.

Systemic administration of **21b** alone resulted in increased CINA levels in liver, kidney, spleen and lymph nodes, compared to control concentrations. Unexpectedly, this effect was additive to LPS only in the liver, where LPS as itself exerted no effect. This may suggest more complex mechanisms for LPS-induced KP activation.

In brain tissue, no significant increase in CINA was detected, suggesting that **21b** is not able to penetrate the blood brain barrier, even if the latter information has never been demonstrated by appropriate assays.

However, these are just preliminary results, that must be confirmed, by repeating the experiments and evaluating what effects **21b** has towards the

levels of other KP metabolites, after LPS-immunization: KYNA, QUIN, 3-HK, and 3-HANA.

## 5.4. Chemistry

Most of the compounds described in this work were synthesized following a common reactions scheme: *I*) modification, if needed, of commercially available synthones (if existent) for the preparation of the appropriate pyridine precursors, *II*) selective oxidation of pyridine nitrogen and *III*) hydrolysis of C<sub>3</sub> substituent (carboxylic ester, cyano group or amide). In this paragraph, all the challenges faced and overcome during the synthetic work and alternative strategies employed to synthesize compounds not accessible *via* the above scheme are reported.

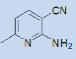
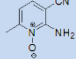
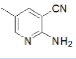
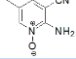
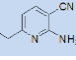
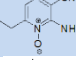
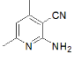
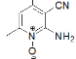
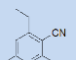
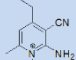
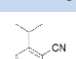
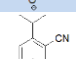
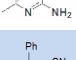
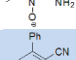
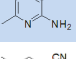
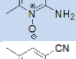
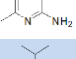
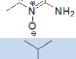
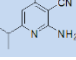
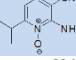
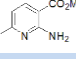
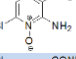
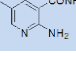
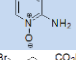
### Oxidation of pyridine nitrogen

Oxidation of pyridine nitrogen was doubtless the key step in all the syntheses (except synthesis of compound **22**). A chemoselective protocol, in order to avoid the concomitant oxidation of 2-amino group or different unexpected side reactions, was necessary. Further, a fast, versatile, high yield procedure, with clean reaction outcome, was pursued, with the aim to produce a library of highly diversified pyridine *N*-oxide derivatives in short time and reducing reaction/purification efforts and costs.

To do this, some of the most exploited N oxidation conditions described in the literature<sup>93</sup> were selected for investigation:

- H<sub>2</sub>O<sub>2</sub>/CH<sub>3</sub>CO<sub>2</sub>H oxidative system,<sup>94</sup>
- oxidation with 3-chloroperoxybenzoic acid (*m*-CIPBA) in chloroform,<sup>95</sup>
- methyltrioxorhenium (MTO) catalysed oxidation in presence of H<sub>2</sub>O<sub>2</sub> in ethanol.<sup>96,97</sup>

Synthetic procedures involving acidic reagents ( $\text{CH}_3\text{CO}_2\text{H}$ , *m*-ClPBA) were not satisfactory for this work, giving raise to complex reaction mixtures, full of by-products and often unworkable. Conversely, MTO catalysed oxidation resulted a mild and powerful protocol for this chemical transformation.

Entry	Pyridine substrate	Reaction time (hours)	Pyridine <i>N</i> -oxide product	Isolated yield
1		1.5		78%
2		1.5		77%
3		1.5		71%
4		1.5		75%
5		1.5		76%
6		1.5		74%
7		3		70%
8		1.5		77%
9		1.5		73%
10		24		70%
11		24		71%
12		24		92% <sup>a)</sup>

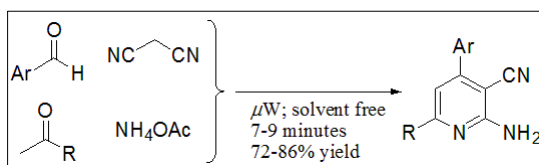
**Table 2.** Summary of the results of MTO catalysed oxidation of pyridine nitrogen in 35% aqueous  $\text{H}_2\text{O}_2$ /ethanol, 1/2. Conditions: substrate/MTO/solvent = 1 mmol/0.10 mmol/4 ml. a) Isolated as a ~92/8 mixture of target product and unreacted starting material; yield calculated by  $^1\text{H}$ -NMR analysis.

Reaction outcomes were very fast and clean: 70-92% yields were achieved in less than 3 hours in all experiments (Table 2, entries 1-9), except for

halogen substituted intermediates (entries 10-12), in which extension of the reaction time to 24 hours was necessary, due to N inactivation by electron-withdrawing halogen atoms, however dropping in the same yield range.

### Microwave assisted multicomponent reaction

In some cases, no pyridine based starting materials were commercially available, so it was necessary to construct *de novo* the 2-aminopyridine ring, with appropriate substituents at the correct positions. Among all the methodologies described in the literature for the synthesis of pyridines,<sup>98</sup> multicomponent reactions (MCRs) are the most attractive, as they are powerful tools to synthesize highly functionalized and asymmetric pyridine derivatives, not infrequently in a “green” fashion.<sup>99</sup> In particular, a microwave accelerated procedure (Scheme 4) has proven very useful for the synthesis of the precursors of several compounds described here.<sup>100</sup>

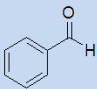
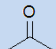
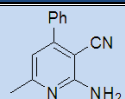
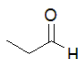
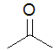
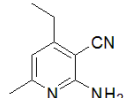
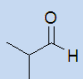
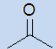
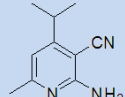
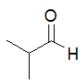
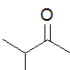
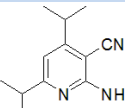
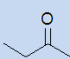
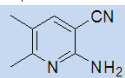


**Scheme 4.** Microwave accelerated one-pot pyridine synthesis in solvent free conditions.

This reaction consists in the one-pot synthesis of 4,6-disubstituted 2-amino-3-cyanopyridine derivatives, from cheap and readily

available starting materials: malononitrile, an aromatic aldehyde, an enolizable ketone (acetone was the only aliphatic ketone described in the original paper) and ammonium acetate as the ammonia source. No catalysts are needed, the transformation occurs in very short times, under solvent free conditions and with simple crystallization from ethanol as the unique purification procedure.

The use of this reaction, apporating slight modifications to the original protocol, gave access to otherwise unavailable starting materials for the synthesis of some of the compounds described in this work. Results are summarized in Table 3.

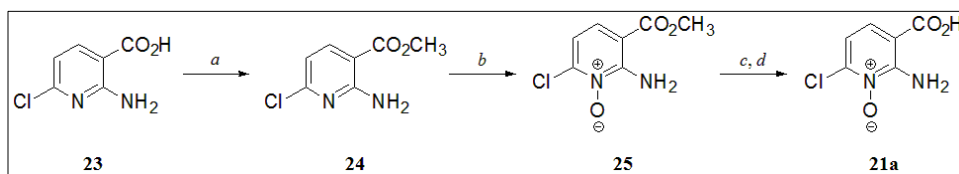
Entry	Substrate aldehyde	Substrate ketone	Product	Isolated yield
1				65%
2				37%
3				40%
4				50%
5	(HCHO) <sub>n</sub>			21% <sup>a)</sup>

**Table 3.** Summary of MCR outcomes. Conditions: malononitrile/aldehyde/ketone/ammonium acetate, 1.00/1.00/1.00/1.50, no solvent, microwave irradiation, 100 °C, 15 minutes. a) Catalyst: AlCl<sub>3</sub>; solvent: <sup>t</sup>BuOH; T = 120 °C; reaction time: 7.5 minutes.

## Syntheses

With this background, all the syntheses of potential 3-HAO inhibitors designed for this project are here described.

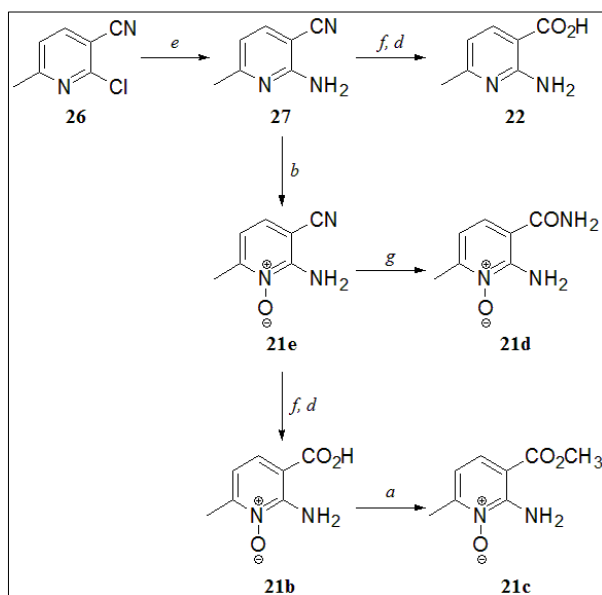
Compound **21a** was obtained from commercially available 6-chloro-2-aminonicotinic acid (**23**), *via* prior conversion in its methyl ester (**24**) by reaction with (trimethylsilyl)diazomethane in toluene/methanol,<sup>101</sup> followed by MTO catalysed oxidation of the pyridine nitrogen and alkaline ester hydrolysis (Scheme 5).



**Scheme 5.** Synthesis of 6-chloro-2-aminonicotinic acid 1-oxide (**21a**). Reagents and conditions: *a*) TMS-diazomethane, toluene/MeOH, 0 °C, 30 minutes, 93% yield; *b*) MTO, 35% aqueous H<sub>2</sub>O<sub>2</sub>, EtOH, r. t., 70% yield; *c*) 10% NaOH in MeOH, reflux, 1 hour; *d*) 3N aqueous HCl, 0 °C, pH 4-5, quantitative yield.

Reaction pathway followed for the synthesis of **21b** allowed to isolate also compounds **21c-e** and **22** (Scheme 6). It started with aromatic amination of commercial 2-chloro-6-methylnicotinonitrile (**26**) with ammonia saturated ethanol,<sup>102</sup> affording **27**. Direct hydrolysis of cyano group<sup>102</sup> of **27** gave **22**. Oxidation of intermediate **27** provided **21e**, which, when completely hydrolysed, led to the synthesis of the most active compound of the series, **21b**. Hydrolysis conditions of **21e** were attenuated, in order to synthesize amide **21d**. This was obtained by simply treating the crude from the oxidative step with saturated aqueous NaHCO<sub>3</sub>, at room temperature. **21c** was obtained by esterification of **21b** following the procedure described for **24**.

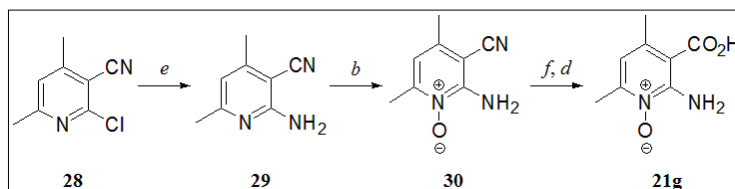




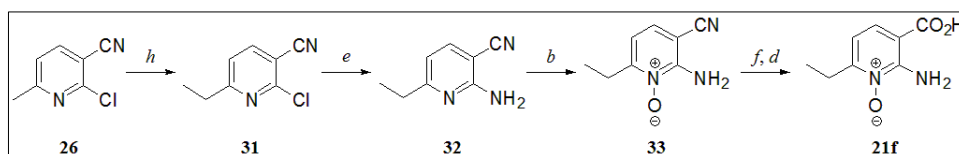
**Scheme 6.** Synthesis of 2-amino-6-methylnicotinic acid (**22**), 2-amino-6-methylnicotinonitrile 1-oxide (**21e**), 2-amino-6-methylnicotinonitrile 1-oxide (**21d**), 2-amino-6-methylnicotinic acid 1-oxide (**21b**), and methyl 2-amino-6-methylnicotinate 1-oxide (**21c**). Reagents and conditions: e)  $\text{NH}_3/\text{EtOH}$ , 160 °C, 24 hours, 85% yield; b) 78% yield; f) 10% aqueous KOH, reflux, 3 hours; d) quantitative yield (for both **22** and **21b**); g) saturated aqueous  $\text{NaHCO}_3$ , r. t., 30 minutes, 90% yield; a) 75% yield.

**21g** was synthesized in the same manner as **21b**, but 2-chloro-4,6-dimethylnicotinonitrile (**28**) was the starting material (Scheme 7).

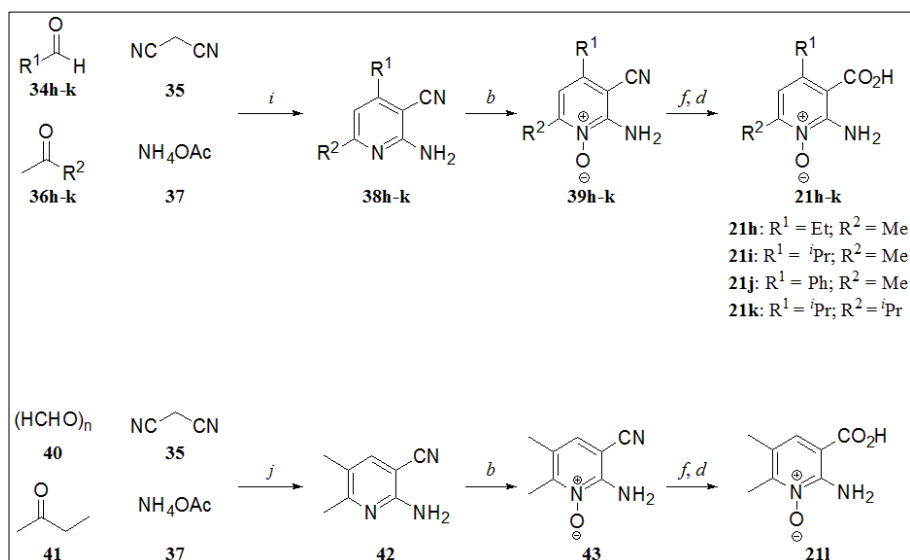
Preparation of **21f** was similar, except for the additional step at the beginning: elongation of the 6-methyl substituent of **26** by reaction with iodomethane in DMF, in presence of sodium hydride (Scheme 8).<sup>102</sup>



**Scheme 7.** Synthesis of 2-amino-4,6-dimethylnicotinic acid 1-oxide (**21g**). Reagents and conditions: e) 83% yield; b) 75% yield; f; d) quantitative yield.



**Scheme 8.** Synthesis of 2-amino-6-ethylnicotinic acid 1-oxide (**21f**). Reagents and conditions: h)  $\text{NaH}$ ,  $\text{CH}_3\text{I}$ , DMF, from 0 °C to r. t., 4 hours, 69% yield; e) 78% yield; b) 71% yield; f; d) quantitative yield.

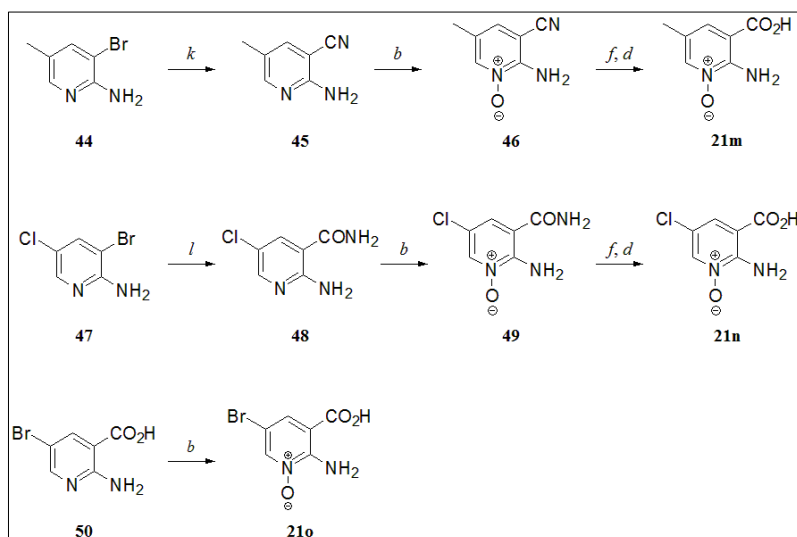


**Scheme 9.** Synthesis of 2-amino-4-ethyl-6-methylnicotinic acid 1-oxide (**21h**), 2-amino-4-isopropyl-6-methylnicotinic acid 1-oxide (**21i**), 2-amino-4-phenyl-6-methylnicotinic acid 1-oxide (**21j**), 2-amino-4,6-diisopropyl-6-methylnicotinic acid 1-oxide (**21k**), and 2-amino-5,6-dimethylnicotinic acid 1-oxide (**21l**). Reagents and conditions: i) microwave irradiation, 100 °C, 15 minutes, 37-65% yield; b) 70-77% yield; f); d) quantitative yield; j) AlCl<sub>3</sub>, *t*BuOH, microwave irradiation, 120 °C, 7.5 minutes, 21% yield.

Above mentioned microwave assisted MCR<sup>100</sup> was exploited to synthesize compounds **21h-l** (Scheme 9).

While **21j** precursor, **38j**, was synthesized using an aromatic aldehyde (benzaldehyde, **34j**) and acetone as the enolizable ketone, like in the original procedure, for precursors of compounds **21h**, **21i** and **21k** only aliphatic reactants were employed, propionaldehyde (**34h**) and acetone, isobutyraldehyde (**34i**) and acetone and isobutyraldehyde (**34k**) and 3-methyl-2-butanone, respectively. Further, synthesis of **21l** precursor, **42**, was performed using paraformaldehyde (**40**) as formaldehyde source and 2-butanone (**41**) as the enolizable ketone. It was necessary to carry the reaction in *tert*-butanol, in order to avoid extensive decomposition and polymerization of highly reactive **40**, and to use a catalytic amount of AlCl<sub>3</sub> to drive the transformation.

**21m** was obtained from commercially available 3-bromo-2-amino-5-methylpyridine (**44**), *via* Pd/DBU catalysed cyanation in presence of potassium hexacyanoferrate(II) trihydrate in *tert*-butanol/water,<sup>103</sup> followed by oxidation of pyridine nitrogen of **45** and nitrile hydrolysis of **46** (Scheme 10). The first step of this synthesis presented the problems of poor conversion of the starting material and hydrolysis of newly formed nitrile to amide, due to the presence of water in the reaction medium. Same pathway was utilized for the synthesis of **21n**, starting from 3-bromo-5-chloro-2-aminopyridine (**47**). The first cyanation step was stressed and performed in microwave conditions in this case, in order to achieve complete starting material consumption and to improve yield of amide **48**, useful intermediate (Scheme 10). Finally, **21o** was obtained *via* direct oxidation of 5-bromo-2-aminonicotinic acid (**50**), affording a 90%+ pure product in one step (Scheme 10).



**Scheme 10.** Synthesis of 2-amino-5-methylnicotinic acid 1-oxide (**21m**), 5-chloro-2-aminonicotinic acid 1-oxide (**21n**) and 5-bromo-2-aminonicotinic acid 1-oxide (**21o**). Reagents and conditions: *k*)  $K_4[Fe(CN)_6] \cdot 3H_2O$ ,  $Pd(PPh_3)_4$ , DBU,  $tBuOH/H_2O$ , 85 °C, 18 hours, 12% yield; *b*) 71-92% yield; *f*); *d*) quantitative yield; *l*)  $K_4[Fe(CN)_6] \cdot 3H_2O$ ,  $Pd(PPh_3)_4$ , DBU,  $tBuOH/H_2O$ , microwave irradiation, 120 °C, 10 minutes, 79% yield.

## Section 6. CONCLUSIONS AND FUTURE PERSPECTIVES

In this PhD project, I was able to design and synthesize a series of 2-aminonicotinic acid 1-oxide derivatives, which represents the first, chemically stable class of 3-HAO inhibitors, not based on the unstable 3-HANA nucleus of previously reported inhibitors. In particular, three compounds, **21a-b** and **21l**, showed interesting 3-HAO inhibitory activity *in vitro* at concentrations lower than 100  $\mu\text{M}$ , with maximum potency registered for **21b**,  $\text{IC}_{50} = 0.6 \mu\text{M}$ . These findings enrich the class of pyridine *N*-oxide based 3-HAO inhibitors, which, before this work, included only 2-aminonicotinic acid 1-oxide, discovered during my Laurea thesis work.

Evaluation of the activity of differently substituted compounds allowed to draw a preliminary SAR profile for this cluster, based on the effect of both electronic and structural properties of substituents around the pyridine ring. Data from biological tests for compounds **21n-o**, which have not yet been tested, will provide an implementation of this preliminary SAR profile. Very interesting, indeed, is the evaluation of the behaviour of an electron withdrawing substituent at position  $\text{C}_5$ , with respect to the electron donating methyl group of **21m**.

Compound **21b** showed activity *in vivo*, where it was able to shift the KP metabolites balance towards the production of neuroprotective agents, after both localized and systemic administration. Thus, this compound represents a relevant starting point to study and validate the hypothesis of the usefulness of “kynurenergic” drugs in the development of novel therapeutic approaches, aimed at interfering with the glutamatergic transmission, in the field of neurodegenerative diseases. In this

framework, particular attention should be addressed at quantifying CNS levels of QUIN, 3-HK and KYNA after **21b** administration in the above mentioned EAE assay. In the case that these data, that will be available soon, will confirm no significant effects on Trp metabolism in the brain, suggesting poor or null blood brain barrier penetration, a specific brain permeability test should be performed and, if negative, optimization of the physical-chemical properties of **21b** will be necessary. It could be achieved by *a*) replacement of the carboxylate with more brain-penetrant bioisosters, e. g. a tetrazole or a nitro group, the latter potentially able, like carboxylate, to bind in a bidentate fashion Arg95 of human 3-HAO, or *b*) use of prodrugs, such as hydrolysable esters. This way could be easily travelled *via* testing *in vivo*, by systemic administration, readily accessible methyl ester **21c**. Investigation of different esters should also be important, because it would allow a fine modulation of the reactivity towards enzymatic hydrolysis in the CNS.

After this physical-chemical optimization, the natural follow-up of the study of the activity of **21b** and its analogues in animal models of MS should be the evaluation of the potential ability of relieving, or even remitting, phenotypic symptoms in chronic EAE rodents.

However, chemical expandability of this class of compounds is still needed. Preliminary docking studies, performed by our group of molecular modelling, suggest some features to be explored, based on the putative positioning of our inhibitor, **21b**, in the active site cleft of human 3-HAO (Figure 12), very similar to that of 4-Cl-3-HANA in the crystal from *Ralstonia metallidurans*.

This study indicates that **21b** shares with 4-Cl-3-HANA the critical binding characteristics: *a*) metal coordination, by *N*-oxide moiety; *b*) Arg95 trapping, in a bidentate fashion, by carboxylate; *c*) H bond network with both Glu53 and Glu105, undertaken by both 2-amino and 1-oxide groups.

Furthermore, deeply analysing the size and the polarity characteristics of the binding pocket, it appears quite clear the possibility to introduce, on the base 2-aminonicotinic acid 1-oxide structure, the following substitutions:

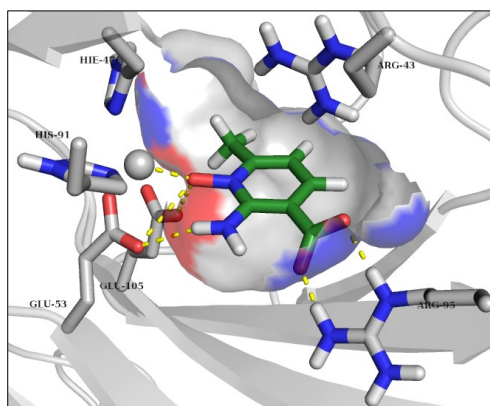


**Figure 12.** Snapshot of the docking of **21b** in the active site of human 3-HAO. Blue surfaces indicate H bond donor residues, red surfaces indicate H bond acceptor residues.

- at the “west side” of 2-aminonicotinic acid 1-oxide core, the size and the shape of the active site surface suggest that there is space for the introduction of a coplanar substituent, with respect to the pyridine ring. Ethinyl substituent at position C<sub>6</sub> seems to fit very well these features and it is the prior candidate to further expand this class of 3-HAO inhibitors;
- additionally, since the above mentioned region of the cleft is surrounded by polar residues, cyano group, which shares planar geometry with ethinyl, but includes a distal polar atom, potentially able to accept H bonds, could be an interesting substitution;
- similarly, hydrophilic residues close to the C<sub>4</sub> position of **21b** can also be targeted by inserting small, polar substituents, such as CH<sub>2</sub>OH, OH, OCH<sub>3</sub>.

Since crystals of human enzyme in complex with inhibitors have never been reported, the crystallization of human 3-HAO bound to **21b** is a very important challenge, because it would be used to validate these preliminary docking model, better understand the mechanism of inhibition of **21b**, and design future inhibitors, possibly endowed with high affinity and selectivity towards the target. NMR studies could also be useful for this purpose, like to unequivocally define the complex catalytic mechanism of this enzyme.

## Section 7. EXPERIMENTAL SECTION (I)

### 7.1. Materials and methods

All compounds were obtained *via* classical synthetic procedures for reaction, purification and characterization, using traditional organic chemistry labwares, at the University of Parma.

Reactants were purchased from both Sigma-Aldrich<sup>®</sup> (Aldrich<sup>®</sup> Chemical Co., Inc., Sigma-Aldrich<sup>®</sup> Corporation, 6000 N. Teutonia Ave., Milwaukee, WI 53209, USA) and Alfa Aesar<sup>®</sup> (Alfa Aesar<sup>®</sup> GmbH & Co., KG, Postbox 110765, 76057 Karlsruhe, Germany) at reagent purity and, unless otherwise noted, used without any previous purification.

Dry solvents used in the reactions were obtained by distillation of technical grade materials over appropriate dehydrating agents.

MCRs were performed using a CEM<sup>®</sup> Microwave Synthesizer - Discover Model.

Reactions were monitored by thin layer chromatography on Kieselgel<sup>®</sup> 60 F 254 (DC-Alufolien, Merck<sup>®</sup>), at both 254 nm and 365 nm wavelengths.

Where indicated, intermediates and final products were purified by silica gel flash chromatography (silica gel, 0.040-0.063 mm), using appropriate solvent mixtures.

Intermediates and final products were characterized by HPLC/MS analysis (HPLC: Agilent<sup>®</sup> 1100 series, equipped with a Waters Symmetry<sup>®</sup> C18, 3.5  $\mu$ m, 4.6 x 75 mm column; MS: Applied Biosystem/MDS SCIEX<sup>®</sup>, with API 150EX<sup>®</sup> ion source, Foster City, CA, USA) and <sup>1</sup>H-NMR analysis (BRUKER AVANCE<sup>®</sup> 300 MHz and BRUKER AVANCE<sup>®</sup> 400



MHz). Where indicated,  $^{13}\text{C}$ -NMR spectra were also recorded. Chemical shifts ( $\delta$  scale) are reported in parts per million (ppm) relative to TMS.  $^1\text{H}$ -NMR spectra are reported in this order: multiplicity and number of protons; signals were characterized as: *s* (singlet), *d* (doublet), *dd* (doublet of doublets), *t* (triplet), *q* (quartet), *hept* (heptaplet), *m* (multiplet), *bs* (broad signal).

## 7.2. Synthetic procedures and characterization of products

### *General procedure for the esterification of nicotinic acids (a).*

(Trimethylsilyl)diazomethane, 2.0 M in diethyl ether (2.00 eq.) was added dropwise, over a period of 15 minutes, to a stirred, cooled (0 °C) suspension of substrate (1.00 eq.) in dry toluene/methanol, 3/2 (v/v, 10 ml/mmol), under a nitrogen atmosphere. The reaction mixture was kept under stirring at this temperature for 30 minutes. At the end of this time, the reaction mixture became a clear, yellow solution. TLC, eluting with chloroform/methanol, 9/1, showed complete consumption of the starting material. The reaction was stopped.

Solvents were evaporated under reduced pressure. The crude, solved in chloroform, was washed with saturated aqueous NaHCO<sub>3</sub> and brine. The organic phase was dried over anhydrous Na<sub>2</sub>SO<sub>4</sub>, filtered and concentrated under reduced pressure. The desired product was purified by silica gel flash chromatography, eluting with chloroform, then chloroform/methanol, 95/5 (yield: 75-93%).

### Methyl 6-chloro-2-aminonicotinate (**24**). Yield: 93%.

<sup>1</sup>H-NMR (DMSO-*d*<sub>6</sub>, 300 MHz)  $\delta$ : 3.82 (s, 3 H), 6.65-6.68 (d, 1 H), 7.54 (bs, 2 H), 8.04-8.07 (d, 1 H).

### Methyl 2-amino-6-methylnicotinate 1-oxide (**21c**). Yield: 75%.

<sup>1</sup>H-NMR (DMSO-*d*<sub>6</sub>, 400 MHz)  $\delta$ : 2.42 (s, 3 H), 3.86 (s, 3 H), 6.75-6.77 (d, 1 H), 7.63-7.65 (d, 1 H), 7.72 (bs, 2 H).

<sup>13</sup>C-NMR (DMSO-*d*<sub>6</sub>, 100.6 MHz)  $\delta$ : 18.78, 52.78, 105.22, 111.76, 127.37, 150.99, 151.81, 166.46.

*General procedure for the oxidation of the pyridine nitrogen (b).*

A 1/2 (v/v) solution of 35% aqueous H<sub>2</sub>O<sub>2</sub> in absolute ethanol was stirred over anhydrous Na<sub>2</sub>SO<sub>4</sub> (5 g/30 ml) at room temperature for 3 hours. After filtration, methyltrioxorhenium(VII) (MTO, 0.10 eq.), followed by substrate (1.00 eq.), was added to this oxidant solution (4 ml/mmol). The reaction mixture was stirred at room temperature for the appropriate time, after which TLC, eluting with chloroform/methanol, 9/1, showed almost complete consumption of the starting material. The reaction was stopped. Brine was added to the reaction mixture and it was extracted with chloroform. The organic phase was dried over anhydrous Na<sub>2</sub>SO<sub>4</sub>, filtered and concentrated under reduced pressure. The desired products, except **21o**, were purified by silica gel flash chromatography, eluting with chloroform, then chloroform/methanol, from 95/5 to 9/1 (yield: 70-78%).

Purification of **21o**: the reaction was stopped by addition of 1N aqueous NaOH. The reaction mixture became an orange solution and it was cooled to 0 °C over an ice bath. 3N aqueous HCl was added dropwise (pH 4-5). A white precipitate immediately formed and it was collected by filtration *in vacuo* in 92% yield.

Methyl 6-chloro-2-aminonicotinate 1-oxide (**25**). Yield: 70%.

<sup>1</sup>H-NMR (DMSO-*d*<sub>6</sub>, 300 MHz)  $\delta$ : 3.87 (*s*, 3 H), 7.02-7.05 (*d*, 1 H), 7.68-7.71 (*d*, 1 H), 7.96 (*bs*, 2 H).

2-Amino-6-methylnicotinonitrile 1-oxide (**21e**). Yield: 78%.

<sup>1</sup>H-NMR (DMSO-*d*<sub>6</sub>, 400 MHz)  $\delta$ : 2.41 (*s*, 3 H), 6.77-6.79 (*d*, 1 H), 7.45-7.47 (*d*, 1 H), 7.71 (*bs*, 2 H).

$^{13}\text{C}$ -NMR (DMSO- $d_6$ , 100.6 MHz)  $\delta$ : 18.65, 89.03, 113.15, 115.95, 129.37, 151.62, 152.61.

2-Amino-4,6-dimethylnicotinonitrile 1-oxide (30). Yield: 75%.

$^1\text{H}$ -NMR (DMSO- $d_6$ , 300 MHz)  $\delta$ : 2.32 (*s*, 3 H), 2.37 (*s*, 3 H), 6.72 (*s*, 1 H), 7.50-7.53 (*d*, 1 H), 7.64 (*bs*, 2 H).

$^{13}\text{C}$ -NMR (DMSO- $d_6$ , 75.5 MHz)  $\delta$ : 18.51, 19.84, 89.93, 114.23, 115.11, 139.90, 150.47, 152.16.

2-Amino-6-ethylnicotinonitrile 1-oxide (33). Yield: 71%.

$^1\text{H}$ -NMR (DMSO- $d_6$ , 300 MHz)  $\delta$ : 1.17-1.22 (*t*, 3 H), 2.78-2.86 (*q*, 2 H), 6.71-6.74 (*d*, 1 H), 7.50-7.53 (*d*, 1 H), 7.75 (*bs*, 2 H).

2-Amino-4-ethyl-6-methylnicotinonitrile 1-oxide (39h). Yield: 76%.

$^1\text{H}$ -NMR ( $\text{CDCl}_3$ , 300 MHz)  $\delta$ : 1.28-1.33 (*t*, 3 H), 2.59 (*s*, 3 H), 2.72-2.80 (*q*, 2 H), 6.43 (*bs*, 2 H), 6.57 (*s*, 1 H).

2-Amino-4-isopropyl-6-methylnicotinonitrile 1-oxide (39i). Yield: 74%.

$^1\text{H}$ -NMR ( $\text{CDCl}_3$ , 300 MHz)  $\delta$ : 1.30-1.32 (*d*, 6 H), 2.59 (*s*, 3 H), 3.14-3.23 (*hept*, 1 H), 6.44 (*bs*, 2 H), 6.58 (*s*, 1 H).

2-Amino-4-phenyl-6-methylnicotinonitrile 1-oxide (39j). Yield: 70%.

$^1\text{H}$ -NMR ( $\text{CD}_3\text{OD}$ , 300 MHz)  $\delta$ : 2.61 (*s*, 3 H), 2.78-2.86 (*q*, 2 H), 6.93 (*s*, 1 H), 7.54-7.56 (*m*, 3 H), 7.64-7.66 (*m*, 2 H).

2-Amino-4,6-diisopropylnicotinonitrile 1-oxide (39k). Yield: 73%.

$^1\text{H}$ -NMR ( $\text{CDCl}_3$ , 300 MHz)  $\delta$ : 1.32-1.33 (*d*, 6 H), 1.32-1.34 (*d*, 6 H), 3.20-3.27 (*hept*, 1 H), 3.77-3.84 (*hept*, 1 H), 6.59 (*bs*, 2 + 1 H).

2-Amino-5,6-dimethylnicotinonitrile 1-oxide (43). Yield: 77%.

$^1\text{H-NMR}$  ( $\text{DMSO-}d_6$ , 400 MHz)  $\delta$ : 2.18 (s, 3 H), 2.40 (s, 3 H), 7.40 (s, 1 H), 7.50 (bs, 2 H).

$^{13}\text{C-NMR}$  ( $\text{DMSO-}d_6$ , 100.6 MHz)  $\delta$ : 15.10, 18.27, 87.86, 116.09, 120.79, 129.77, 150.87, 151.10.

2-Amino-5-methylnicotinonitrile 1-oxide (46). Yield: 77%.

$^1\text{H-NMR}$  ( $\text{DMSO-}d_6$ , 400 MHz)  $\delta$ : 2.13 (s, 3 H), 7.46 (s, 1 H), 7.50 (bs, 2 H), 8.30 (s, 1 H).

$^{13}\text{C-NMR}$  ( $\text{DMSO-}d_6$ , 100.6 MHz)  $\delta$ : 16.88, 91.37, 115.71, 122.15, 131.43, 141.18, 150.83.

5-Chloro-2-aminonicotinamide 1-oxide (49). Yield: 71%.

$^1\text{H-NMR}$  ( $\text{DMSO-}d_6$ , 300 MHz)  $\delta$ : 7.77 (s, 1 H), 7.84 (s, 3 H), 8.23 (s, 1 H), 8.55 (s, 1 H).

5-Bromo-2-aminonicotinic acid 1-oxide (21o). Yield: 92%.

$^1\text{H-NMR}$  ( $\text{DMSO-}d_6$ , 300 MHz)  $\delta$ : 7.77 (bs, 3 H), 7.80 (s, 1 H), 8.66 (s, 1 H), 13.77 (bs, 1 H).

6-Chloro-2-aminonicotinic acid 1-oxide (21a).

A fine suspension of methyl 6-chloro-2-aminonicotinate 1-oxide (**25**) in 10% NaOH in methanol (1 ml/mmol) was heated to reflux and stirred at this temperature for 1 hour. TLC after this time, eluting with chloroform/ethanol/formic acid, 8.7/1.0/0.3, showed complete consumption of the starting material. The reaction was stopped.

After cooling to room temperature, methanol was removed by evaporation *in vacuo*. The crude, white solid was solved in minimum amount of water. The clear, colourless solution so obtained was cooled to 0 °C and carefully

acidified to pH 4-5, with 3N aqueous HCl. A white precipitate immediately formed. The desired product was collected by filtration *in vacuo* in quantitative yield.

$^1\text{H-NMR}$  (DMSO- $d_6$ , 300 MHz)  $\delta$ : 7.00-7.03 (*d*, 1 H), 7.67-7.70 (*d*, 1 H), 7.95 (*bs*, 2 H).

*General procedure for the amination of 2-chloropyridines (e).*

A solution of the substrate in ethanol saturated with ammonia (1 ml/mmol) was placed in a sealed steel bomb, heated to 160 °C and maintained at this temperature for 24 hours. After cooling to room temperature, solvent was removed by evaporation *in vacuo* and the desired product was purified by silica gel flash chromatography, eluting with chloroform/methanol, from 99/1 to 95/5 (yield: 78-85%).

2-Amino-6-methylnicotinonitrile (27). Yield: 85%.

$^1\text{H-NMR}$  (DMSO- $d_6$ , 300 MHz)  $\delta$ : 2.30 (*s*, 3 H), 6.50-6.53 (*d*, 1 H), 6.76 (*bs*, 2 H), 7.70-7.73 (*d*, 1 H).

$^{13}\text{C-NMR}$  (DMSO- $d_6$ , 75.5 MHz)  $\delta$ : 24.31, 86.10, 111.58, 117.36, 142.09, 159.55, 162.57.

2-Amino-6-ethylnicotinonitrile (32). Yield: 78%.

$^1\text{H-NMR}$  (CDCl<sub>3</sub>, 400 MHz)  $\delta$ : 1.25-1.28 (*t*, 3 H), 2.65-2.71 (*q*, 2 H), 5.30 (*bs*, 2 H), 6.58-6.60 (*d*, 1 H), 7.60-7.62 (*d*, 1 H).

$^{13}\text{C-NMR}$  (CDCl<sub>3</sub>, 100.6 MHz)  $\delta$ : 13.12, 31.49, 107.65, 115.03, 120.77, 142.58, 151.97, 169.01.

2-Amino-4,6-dimethylnicotinonitrile (29). Yield: 83%.

$^1\text{H-NMR}$  (CDCl<sub>3</sub>, 300 MHz)  $\delta$ : 2.39 (*s*, 3 H), 2.40 (*s*, 3 H), 5.15 (*bs*, 2 H), 6.47 (*s*, 1 H).

*General procedure for the hydrolysis of nitriles and 5-chloro-2-aminonicotinamide 1-oxide (49) to the corresponding carboxylic acids (f, d).*

A fine suspension of the substrate in 10% aqueous KOH (1 ml/mmol) was heated to reflux and stirred at this temperature for 3 hours. TLC after this time, eluting with chloroform/ethanol/formic acid, 8.7/1.0/0.3, showed complete consumption of the starting material. The reaction was stopped. After cooling to room temperature, the clear, colourless solution so obtained was cooled to 0 °C and carefully acidified to pH 4-5, with 3N aqueous HCl. A white precipitate immediately formed. The desired product was collected by filtration *in vacuo* in quantitative yield.

2-Amino-6-methylnicotinic acid 1-oxide (21b).

<sup>1</sup>H-NMR (DMSO-*d*<sub>6</sub>, 300 MHz)  $\delta$ : 2.42 (*s*, 3 H), 6.71-6.74 (*d*, 1 H), 7.62-7.65 (*d*, 1 H), 7.72 (*bs*, 2 H), 13.42 (*bs*, 1 H).

<sup>13</sup>C-NMR (DMSO-*d*<sub>6</sub>, 75.5 MHz)  $\delta$ : 18.78, 106.34, 111.55, 128.02, 150.70, 152.12, 168.10.

2-Amino-6-methylnicotinic acid (22).

<sup>1</sup>H-NMR (DMSO-*d*<sub>6</sub>, 300 MHz)  $\delta$ : 2.30 (*s*, 3 H), 6.46-6.49 (*d*, 1 H), 7.16 (*bs*, 2 H), 7.91-7.93 (*d*, 1 H).

<sup>13</sup>C-NMR (DMSO-*d*<sub>6</sub>, 75.5 MHz)  $\delta$ : 24.10, 102.71, 111.37, 140.34, 159.31, 162.57, 168.59.

2-Amino-4,6-dimethylnicotinic acid 1-oxide (21g).

<sup>1</sup>H-NMR (DMSO-*d*<sub>6</sub>, 300 MHz)  $\delta$ : 2.44 (*s*, 2 x 3 H), 6.73 (*s*, 1 H), 8.04 (*bs*, 2 H).

$^{13}\text{C}$ -NMR (DMSO- $d_6$ , 75.5 MHz)  $\delta$ : 18.14, 22.60, 109.64, 115.27, 146.47, 149.40, 151.81, 167.73.

2-Amino-6-ethylnicotinic acid 1-oxide (21f).

$^1\text{H}$ -NMR (DMSO- $d_6$ , 400 MHz)  $\delta$ : 1.19-1.23 (*t*, 3 H), 2.82-2.85 (*q*, 2 H), 6.66-6.69 (*d*, 1 H), 7.66-7.68 (*d*, 1 H), 7.75 (*bs*, 2 H), 13.49 (*bs*, 1 H).

$^{13}\text{C}$ -NMR (DMSO- $d_6$ , 100.6 MHz)  $\delta$ : 10.87, 24.63, 109.56, 128.19, 152.12, 154.74, 168.22.

2-Amino-4-ethyl-6-methylnicotinic acid 1-oxide (21h).

$^1\text{H}$ -NMR (DMSO- $d_6$ , 300 MHz)  $\delta$ : 1.05-1.10 (*t*, 3 H), 2.28 (*s*, 3 H), 2.81-2.88 (*q*, 2 H), 6.38 (*s*, 1 H), 7.39 (*bs*, 2 H).

2-Amino-4-isopropyl-6-methylnicotinic acid 1-oxide (21i).

$^1\text{H}$ -NMR (DMSO- $d_6$ , 300 MHz)  $\delta$ : 1.08-1.10 (*d*, 6 H), 2.31 (*s*, 3 H), 3.38 (*hept*, 1 H), 6.51 (*s*, 1 H), 6.99 (*bs*, 2 H).

2-Amino-4-phenyl-6-methylnicotinic acid 1-oxide (21j).

$^1\text{H}$ -NMR (CD $_3$ OD, 300 MHz)  $\delta$ : 2.58 (*s*, 3 H), 6.75 (*s*, 1 H), 7.35-7.43 (*m*, 5 H).

2-Amino-4,6-diisopropylnicotinic acid 1-oxide (21k).

$^1\text{H}$ -NMR (CD $_3$ OD, 300 MHz)  $\delta$ : 1.26-1.28 (*d*, 6 H), 1.33-1.35 (*d*, 6 H), 3.65-3.74 (*m*, 2 H), 6.74 (*s*, 1 H).

2-Amino-5,6-dimethylnicotinic acid 1-oxide (21l).

$^1\text{H}$ -NMR (DMSO- $d_6$ , 400 MHz)  $\delta$ : 2.21 (*s*, 3 H), 2.42 (*s*, 3 H), 7.52 (*bs*, 2 H), 7.55 (*s*, 1 H), 13.25 (*bs*, 1 H).

$^{13}\text{C}$ -NMR (DMSO- $d_6$ , 100.6 MHz)  $\delta$ : 15.17, 18.48, 105.42, 118.68, 128.74, 149.83, 150.33, 168.09.



2-Amino-5-methylnicotinic acid 1-oxide (**21m**).

<sup>1</sup>H-NMR (DMSO-*d*<sub>6</sub>, 400 MHz)  $\delta$ : 2.16 (s, 3 H), 7.47 (bs, 2 H), 7.59 (s, 1 H), 8.24 (s, 1 H).

<sup>13</sup>C-NMR (DMSO-*d*<sub>6</sub>, 100.6 MHz)  $\delta$ : 17.11, 108.71, 120.18, 130.06, 140.30, 150.20, 167.78.

5-Chloro-2-aminonicotinic acid 1-oxide (**21n**).

<sup>1</sup>H-NMR (DMSO-*d*<sub>6</sub>, 300 MHz)  $\delta$ : 7.71 (s, 1 H), 7.77 (bs, 2 H), 8.61 (s, 1 H).

2-Amino-6-methylnicotinamide 1-oxide (**21d**).

A mixture of 2-amino-6-methylnicotinonitrile 1-oxide (**21e**) and saturated aqueous NaHCO<sub>3</sub> (10 ml/mmol) was stirred at room temperature for 30 minutes. TLC after this time, eluting with chloroform/methanol, 9/1, showed almost complete consumption of the starting material. The reaction was stopped.

The reaction mixture was extracted with chloroform. The organic phase was washed with brine, dried over anhydrous Na<sub>2</sub>SO<sub>4</sub>, filtered and concentrated under reduced pressure. The crude was purified by silica gel flash chromatography, eluting with chloroform/methanol, from 95/5 to 85/15, affording pure, target product in 90% yield, as a light brown powder.

<sup>1</sup>H-NMR (DMSO-*d*<sub>6</sub>, 300 MHz)  $\delta$ : 2.39 (s, 3 H), 6.69-6.71 (d, 1 H), 7.55 (bs, 1 H), 7.59-7.62 (d, 1 H), 7.85 (bs, 2 H), 8.09 (bs, 1 H).

<sup>13</sup>C-NMR (DMSO-*d*<sub>6</sub>, 75.5 MHz)  $\delta$ : 18.05, 108.22, 110.39, 124.89, 148.57, 151.12, 168.45.

2-Chloro-6-ethylnicotinonitrile (31).

Sodium hydride, 60% dispersion in mineral oil (1.50 eq.), was carefully added, under a nitrogen atmosphere, to a stirred, cooled (0 °C) solution of 2-chloro-6-methylnicotinonitrile (**26**, 1.00 eq.) in dry *N,N*-dimethylformamide (2.5 ml/mmol). After stirring at this temperature for 15 minutes, iodomethane (4.00 eq.) was added. The reaction mixture was allowed to warm to room temperature and stirred for 4 hours under nitrogen. TLC after this time, eluting with petroleum ether/ethyl acetate, 7/3, showed almost complete consumption of the starting material. The reaction was stopped.

The reaction mixture was cooled to 0 °C, then water was carefully added. The mixture was extracted with diethyl ether. The organic phase was washed with brine, dried over anhydrous Na<sub>2</sub>SO<sub>4</sub>, filtered and concentrated under reduced pressure. The crude was purified by silica gel flash chromatography, eluting with petroleum ether/ethyl acetate, from 9/1 to 8/2, affording the target product in 69% yield, as a colourless oil.

<sup>1</sup>H-NMR (CHCl<sub>3</sub>, 400 MHz)  $\delta$ : 1.29-1.33 (*t*, 3 H), 2.85-2.90 (*q*, 2 H), 7.24-7.26 (*d*, 1 H), 7.90-7.92 (*d*, 1 H).

<sup>13</sup>C-NMR (CHCl<sub>3</sub>, 100.6 MHz)  $\delta$ : 13.12, 31.49, 107.65, 115.03, 120.77, 142.58, 151.97, 169.01.

*General procedure for the multicomponent reaction (i).*

A 10 ml microwave tube was charged with malononitrile (1.00 eq.), appropriate aldehyde (1.00 eq.), appropriate ketone (1.00 eq.) and ammonium acetate (1.50 eq.). The tube was placed in a microwave oven and irradiated at 100 °C for 15 minutes, with a maximum power output of 150 W. The resulting crude was purified by silica gel flash

chromatography, eluting with appropriate petroleum ether/ethyl acetate mixtures, affording the target products in 37-65% yield.

2-Amino-4-ethyl-6-methylnicotinonitrile (**38h**). Yield: 37%.

<sup>1</sup>H-NMR (CDCl<sub>3</sub>, 300 MHz)  $\delta$ : 1.26-1.30 (*t*, 3 H), 2.40 (*s*, 3 H), 2.69.2.75 (*q*, 1 H), 5.20 (*bs*, s H), 6.48 (*s*, 1 H).

2-Amino-4-isopropyl-6-methylnicotinonitrile (**38i**). Yield: 40%.

<sup>1</sup>H-NMR (DMSO-*d*<sub>6</sub>, 300 MHz)  $\delta$ : 1.17-1.20 (*d*, 6 H), 2.29 (*s*, 3 H), 2.95-3.04 (*hept*, 1 H), 6.51 (*s*, 1 H), 6.67 (*bs*, s H).

2-Amino-4-phenyl-6-methylnicotinonitrile (**38j**). Yield: 65%.

<sup>1</sup>H-NMR (DMSO-*d*<sub>6</sub>, 300 MHz)  $\delta$ : 2.35 (*s*, 3 H), 6.59 (*s*, 1 H), 6.89 (*bs*, 2 H), 7.50-7.56 (*m*, 5 H).

2-Amino-4,6-diisopropylnicotinonitrile (**38k**). Yield: 50%.

<sup>1</sup>H-NMR (CDCl<sub>3</sub>, 300 MHz)  $\delta$ : 1.24-1.28 (*d*, 6 H), 1.27-1.31 (*d*, 6 H), 2.81-2.95 (*hept*, 1 H), 3.11-3.23 (*hept*, 1 H), 5.18 (*bs*, 2 H), 6.51 (*s*, 1 H).

2-Amino-5,6-dimethylnicotinonitrile (**42**).

A 10 ml microwave tube was charged with a mixture of malononitrile (1.00 eq.), paraformaldehyde (1.00 eq.), 2-butanone (1.00 eq.), ammonium acetate (1.50 eq.) and AlCl<sub>3</sub> (0.05 eq.) in *tert*-butanol (0.5 ml/mmol). The tube was placed in a microwave oven and irradiated at 120 °C for 7.5 minutes, with a maximum power output of 250 W.

After cooling to room temperature, solvent was removed by evaporation *in vacuo* and the crude was purified by silica gel flash chromatography, eluting with petroleum ether/ethyl acetate, from 9/1 to 6/4, affording the pure, target product in 21% yield.

$^1\text{H-NMR}$  (DMSO- $d_6$ , 400 MHz)  $\delta$ : 2.07 (*s*, 3 H), 2.28 (*s*, 3 H), 6.51 (*bs*, 2 H), 7.57 (*s*, 1 H).

$^{13}\text{C-NMR}$  (DMSO- $d_6$ , 100.6 MHz)  $\delta$ : 17.46, 23.01, 86.61, 117.93, 119.70, 142.26, 158.53, 161.86.

### 2-Amino-5-methylnicotinonitrile (45).

A mixture of 3-bromo-2-amino-5-methylpyridine (**44**, 1.00 eq.), potassium hexacyanoferrate(II) trihydrate  $\{\text{K}_4[\text{Fe}(\text{CN})_6]\cdot 3\text{H}_2\text{O}$ , 0.40 eq.}, tetrakis(triphenylphosphine)palladium(0)  $[\text{Pd}(\text{PPh}_3)_4$ , 0.05 eq.] and 1,8-diazabicyclo[5.4.0]undec-7-ene (DBU, 0.25 eq.) in *tert*-butanol/water, 1/1 (*v/v*, 3 ml/mmol) was heated to 85 °C and stirred at this temperature for 18 hours. TLC after this time, eluting with chloroform/methanol, 95/5, showed not complete consumption of the starting material. The reaction was stopped.

The reaction mixture was extracted with ethyl acetate. The organic phase was washed with brine, dried over anhydrous  $\text{Na}_2\text{SO}_4$ , filtered and concentrated under reduced pressure. The crude was purified by silica gel flash chromatography, eluting with petroleum ether/ethyl acetate, from 8/2 to 7/3, affording pure, target product in 12% yield, as a white powder. Starting material was recovered in 78% yield.

$^1\text{H-NMR}$  (DMSO- $d_6$ , 400 MHz)  $\delta$ : 2.12 (*s*, 3 H), 6.61 (*bs*, 2 H), 7.69-7.70 (*d*, 1 H), 8.06-8.07 (*d*, 1 H).

$^{13}\text{C-NMR}$  (DMSO- $d_6$ , 100.6 MHz)  $\delta$ : 16.81, 89.28, 117.60, 121.12, 142.30, 153.79, 158.78.

### 5-Chloro-2-aminonicotinamide (48).

A 10 ml microwave tube was charged with a mixture of 3-bromo-5-chloro-2-aminopyridine (**47**, 1.00 eq.), potassium hexacyanoferrate(II) trihydrate  $\{K_4[Fe(CN)_6] \cdot 3H_2O$ , 0.40 eq.}, tetrakis(triphenylphosphine)palladium(0)  $[Pd(PPh_3)_4$ , 0.05 eq.] and 1,8-diazabicyclo[5.4.0]undec-7-ene (DBU, 0.25 eq.) in *tert*-butanol/water, 1/1 (v/v, 3 ml/mmol). The tube was placed in a microwave oven and irradiated at 120 °C for 10 minutes, with a maximum power output of 250 W. TLC after this time, eluting with chloroform/methanol, 95/5, showed complete consumption of the starting material.

Brine was added to the reaction mixture and it was extracted with chloroform. The organic phase was washed with brine, dried over anhydrous  $Na_2SO_4$ , filtered and concentrated under reduced pressure. The crude was purified by filtration over a pad of silica gel, washing with petroleum ether/ethyl acetate, 1/1, then chloroform/methanol, 9/1. The desired product was isolated in 79% yield, as a yellow powder.

$^1H$ -NMR ( $DMSO-d_6$ , 400 MHz)  $\delta$ : 7.35 (*bs*, 2 H), 7.46 (*bs*, 1 H), 8.05-8.10 (*m*, 3 H).

## Section 8. DIAZO CHEMISTRY

During the second year of my doctorate I worked at the Dipartimento di Chimica e Tecnologia del Farmaco - Università di Perugia.

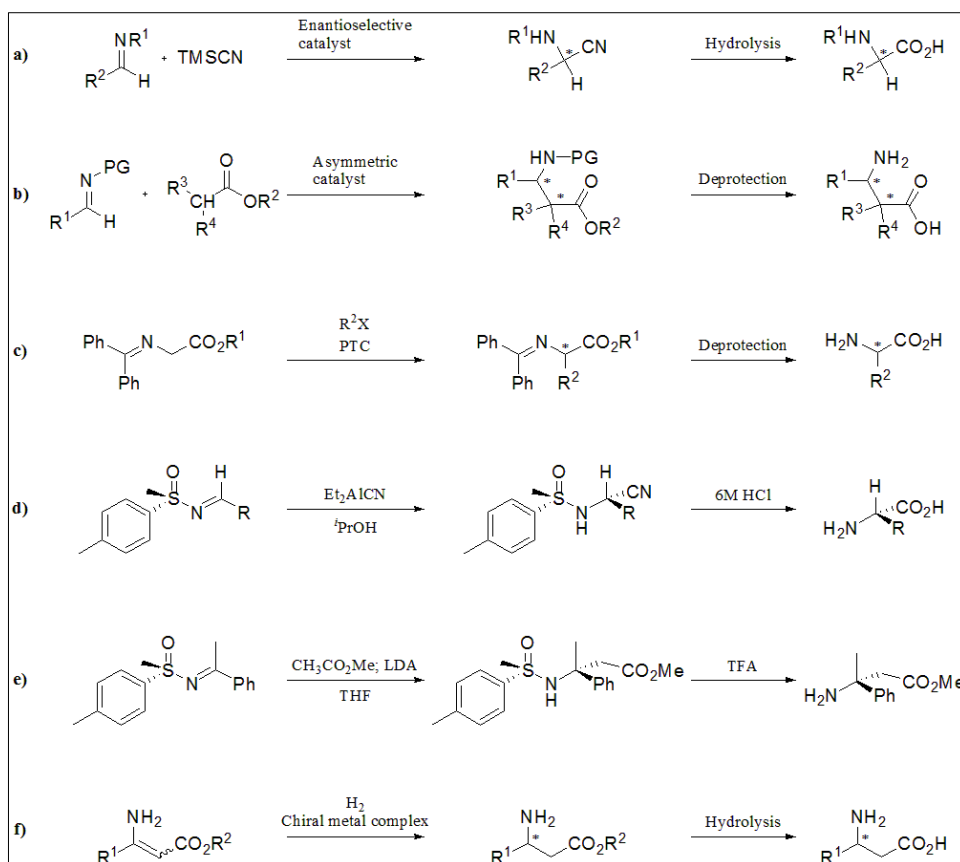
Under the supervision of Prof. Pellicciari and Antimo Gioiello, PhD, I was involved in an organic chemistry project, aimed at further exploring the reactivity of  $\alpha$ -dialzo- $\beta$ -hydroxyesters towards Lewis acid-induced decomposition, and at evaluating the synthetic utility of this reaction.

In particular, my work was to carry on the investigation about boron trifluoride diethyletherate ( $\text{BF}_3 \cdot \text{Et}_2\text{O}$ )-induced decomposition of 2-dialzo-3-hydroxy-3-phenyl-3-alkylpropanoates in acetonitrile.

Since the outcome of this reaction is the *de novo* synthesis of amino acids precursors, a brief overview on traditional and recent methods for the synthesis of amino acids is reported in this section, followed by the description of the state of the art of the knowledge about Lewis acid-induced decomposition of  $\alpha$ -dialzocarbonyl compounds.

## 8.1. Synthesis of amino acids

Due to the biological relevance of amino acids, organic chemists have always been engaged in developing useful procedures to easily prepare both natural and non-natural amino acids, preferably in enantiopure form.<sup>104,105</sup>



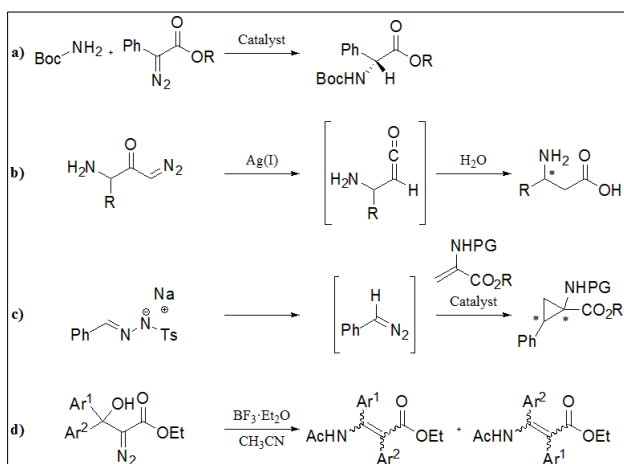
**Scheme 11.** Summary of recent asymmetric amino acids synthesis methods. **a)** Strecker synthesis of  $\alpha$ -amino acids; **b)** use of the Mannich reaction for the synthesis of  $\beta$ -amino acids; **c)** reaction of glycine enolates with electrophiles under PTC conditions; **d)** synthesis of  $\alpha$ -amino acids from sulfinimines; **e)** synthesis of  $\beta$ -phenylalanine methyl ester from sulfinimines; **f)** catalytic asymmetric hydrogenation of enaminoesters.

Among the wide literature thereupon, classical “name reactions”, like the Strecker synthesis of  $\alpha$ -amino acids and the Mannich reaction, leading to  $\beta$ -amino acids, and their asymmetric versions are still the most

exploited.<sup>106,107</sup> Besides these traditional methods, reactions of glycine enolates with electrophiles under chiral phase transfer catalyst (PTC) conditions,<sup>108</sup> sulfinimines chemistry<sup>109</sup> and catalytic asymmetric hydrogenation of enaminoesters<sup>110</sup> are useful synthetic tools to obtain biologically interesting chiral  $\alpha$ - and  $\beta$ -amino acids (Scheme 11). The versatile chemistry of  $\alpha$ -diazocarbonyl compounds<sup>111</sup> adds to these procedures, making possible the solution of complex synthetic issues.

Diazo reactants have been successfully employed in several ways for the synthesis of amino acids (Scheme 12):

- *via* asymmetric N-H insertion of  $\alpha$ -diazoesters into Boc-protected amines;<sup>112</sup>
- exploiting the Wolff rearrangement in the one carbon homologation of  $\alpha$ -amino acids *via* the corresponding  $\alpha$ -diazoketones;<sup>113</sup>
- in diastereoselective cyclopropanation reactions, leading to cyclopropane  $\alpha$ -amino acids.<sup>114</sup>



**Scheme 12.** Diazo synthesis of amino acids. **a)** N-H insertion reaction of  $\alpha$ -diazoesters and carbamates; **b)** Wolff rearrangement-induced homologation of  $\alpha$ -amino acids into  $\beta$ -amino acids; **c)** cyclopropanation of olefines; **d)** Lewis acid-induced decomposition of  $\alpha$ -diazo- $\beta$ -hydroxyesters in acetonitrile, leading to  $\beta$ -enaminoesters.

Recently, the discovery that the Lewis acid-induced decomposition of easily prepared  $\alpha$ -diazo- $\beta$ -hydroxyesters afforded  $\alpha$ - and  $\beta$ -enaminoesters in moderate to high yields<sup>115,116</sup> provided to

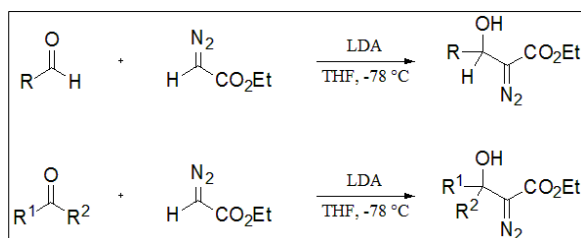


organic chemists a new, versatile method to walk the route to amino acids synthesis.

This reaction will be discussed in detail in the following pages.

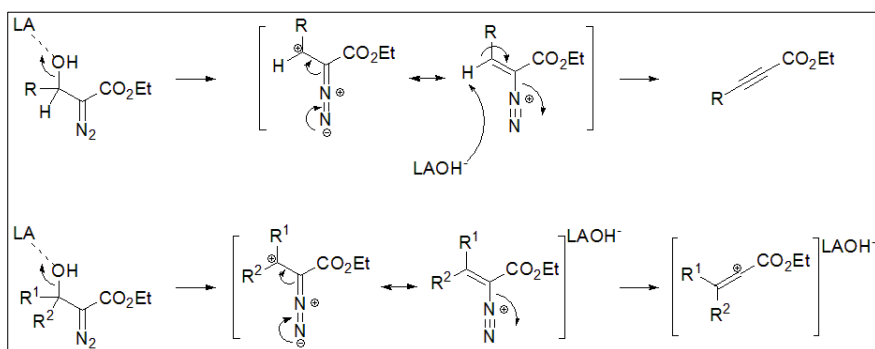
## 8.2. Lewis acid-induced decomposition of $\alpha$ -diazo- $\beta$ -hydroxyesters

Reaction between ethyl diazoacetate (EDA) and carbonyl compounds in aldol conditions provides synthetically useful  $\alpha$ -diazo- $\beta$ -hydroxyesters (Scheme 13).<sup>117</sup>



**Scheme 13.** Aldol type reaction between EDA and carbonyl compounds. LDA: lithium diisopropylamide.

Treating these intermediates with Lewis acids causes decomposition and results in the formation of an array of products, depending on the nature of the carbonyl precursor (aldehyde or ketone), the conditions employed (solvent) and the properties of substituents (alkyl or aryl, cyclic or acyclic, electron rich or electron deficient groups).<sup>115,116,118,119</sup> Although different Lewis acids are suitable reagents for these transformations,  $\text{BF}_3 \cdot \text{Et}_2\text{O}$  is the most exploited one, and allows to obtain the most synthetically useful products.



**Scheme 14.** General mechanism of the Lewis acid-induced decomposition of  $\alpha$ -diazo- $\beta$ -hydroxyesters derived from aldehydes (top) or ketones (bottom). LA: Lewis acid.

In all cases, the reaction proceeds *via* OH coordination and extrusion by the Lewis acid, leading to a highly unstable cation, which bears the best leaving group known in organic chemistry, molecular nitrogen (Scheme 14).

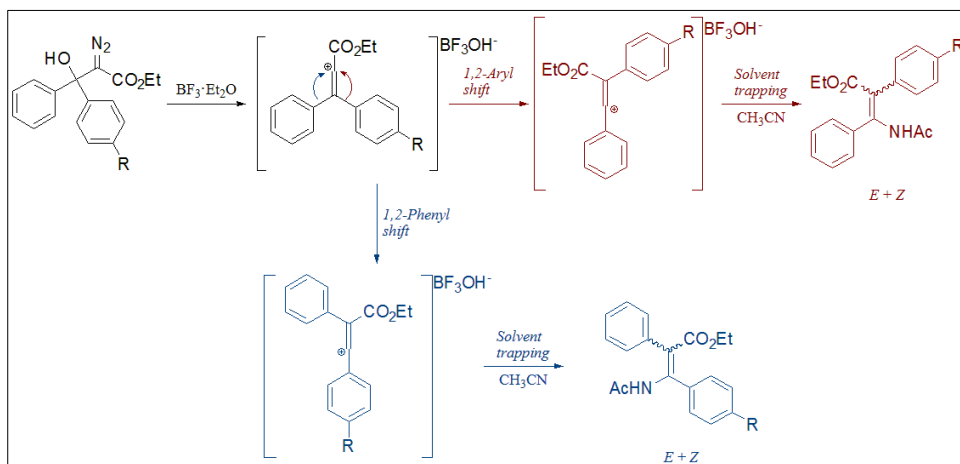
When the carbonyl precursor is an aldehyde, the availability of a proton bound to the positively charged carbon atom allows deprotonation which, combined with nitrogen loss, leads to the formation of a 2-ynoate derivative.<sup>120</sup>

On the other hand, direct nitrogen loss from ketones-derived cations affords a key, highly reactive intermediate, vinyl cation, which rapidly follows complex rearrangement pathways, giving the most diverse products.

Rearrangement of so formed vinyl cations was investigated by performing the decomposition reaction with  $\text{BF}_3 \cdot \text{Et}_2\text{O}$  in different solvents and, once identified acetonitrile as the solvent of choice, giving the greatest product diversity,<sup>115</sup> by reacting ethyl  $\alpha$ -diazo- $\beta$ -hydroxy- $\beta$ -phenylpropanoate derivatives substituted at position  $\text{C}_3$  with aryl groups, diverse in the electronic properties of substituents on the aromatic ring (Scheme 15).<sup>116</sup>

In particular, reaction of 2-diazo-3-hydroxy-3-aryl-3-phenylpropanoates with a stoichiometric amount of  $\text{BF}_3 \cdot \text{Et}_2\text{O}$  in acetonitrile afforded the expected isomeric  $\beta$ -enaminoesters as the only products, *via* Lewis acid-induced formation of the vinyl cation and 1,2-aryl or 1,2-phenyl migration, followed by solvent trapping. The propensity for 1,2-aryl shift, in the process of stabilization of the intermediate vinyl cation has been proposed to be strongly related to the electron density of the aryl ring,

given by the C<sub>4</sub> substituent: migration of electron enriched aryl groups is favoured (*p*-NO<sub>2</sub> vs *p*-OMe, Table 4, entries 2-3).



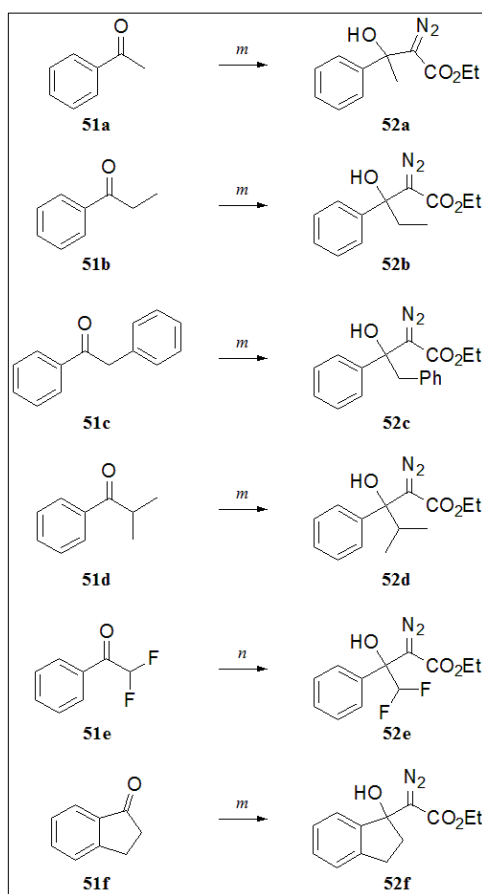
**Scheme 15.** Mechanism of the BF<sub>3</sub>·Et<sub>2</sub>O-induced decomposition of 2-diazo-3-hydroxy-3-aryl-3-phenylpropanoates in acetonitrile.

Entry	R	Combined isolated yields of $\beta$ -enaminoesters	Aryl shift/Phenyl shift
1	H	90%	-
2	NO <sub>2</sub>	87%	43 / 57
3	OMe	90%	76 / 24
4	Cl	92%	58 / 42
5	Me	97%	54 / 46
6	F	88%	60 / 40

**Table 4.** Comparison between 1,2-aryl shift and 1,2-phenyl shift yields of the BF<sub>3</sub>·Et<sub>2</sub>O-induced decomposition of different 2-diazo-3-hydroxy-3-aryl-3-phenylpropanoates in acetonitrile.

These results open the road to further investigations on the relative stability of vinyl cations, particularly those deriving from the decomposition of alkyl-substituted  $\alpha$ -diazo- $\beta$ -hydroxyesters.

### 8.3. $\text{BF}_3 \cdot \text{Et}_2\text{O}$ -induced decomposition of 2-diazo-3-hydroxy-3-phenyl-3-alkylpropanoates in acetonitrile



**Scheme 16.** Synthesis of ethyl 2-diazo-3-hydroxy-3-phenyl-3-alkylpropanoates **52a-f**. Reagents and conditions: *m*) LDA, EDA, THF, -78 °C, 2 hours, 71-91% yield; *n*) 30 minutes, 80% yield.

In order to proceed the investigation on the effect of the electronic properties of  $\beta$ -substituents, regarding the outcome of the Lewis acid-induced decomposition of  $\alpha$ -diazo- $\beta$ -hydroxyesters in acetonitrile, and to find novel synthetic applications to this reaction, a series of ethyl 2-diazo-3-hydroxy-3-phenyl-3-alkylpropanoates, **52a-f**, was synthesized, by aldol type condensation between ethyl diazoacetate and appropriate acetophenone derivatives **51a-f**

(Scheme 16). These intermediates were then decomposed in previously

reported conditions and all the products obtained were isolated and characterized.

Data analysis allowed to speculate on the influence of the electronic properties of  $\beta$ -alkyl substituents, as well as on the complex mechanisms behind the formation of unexpected products.

### Synthesis of $\alpha$ -diazo- $\beta$ -hydroxyesters and Lewis acid-induced decomposition

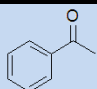
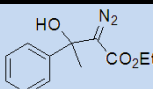
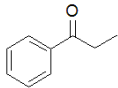
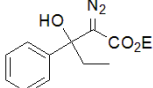
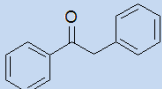
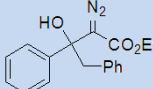
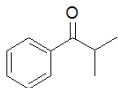
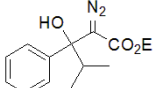
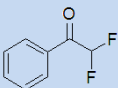
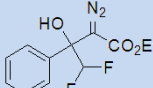
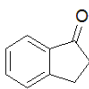
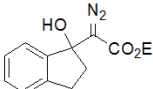
Compounds **52a-b** were obtained in 87% and 91% yield (Table 5, entries 1 and 2), respectively, using classical conditions of the aldol type condensation (method A): slow addition of a cold (-78 °C) solution of LDA, generated *in situ*, in THF to a solution of EDA and appropriate ketone in THF, at -78 °C, then aqueous quenching of the reaction mixture after completion and filtration of the crude on a pad of alumina.

This procedure was not effective for the synthesis of compounds **52c-d** and **52f**, that were isolated in low yields following this protocol. However, optimization of the quenching conditions, by adding a cold (-78 °C), diluted solution of acetic acid in THF, led to improved yields and allowed to obtain desired diazo compounds in 82%, 76% and 71% yield, respectively (method B, entries 3, 4 and 6).

Furthermore, an expedient was implemented in the synthesis of compound **52e**, in order to avoid unwanted side reactions, due to the expected high reactivity of di-fluorinated precursor **51e**. Thus, prior LDA mediated lithiation of EDA, subsequent addition of a solution of **51e** in THF at -78 °C and acetic acid quenching afforded product **52e** in 80% isolated yield (method C, entry 5).

Therefore, the Lewis acid-induced decomposition of  $\alpha$ -diazo- $\beta$ -hydroxyesters thus formed in acetonitrile was studied. According to the

set-up protocol, a solution of compounds **52a-f** in dry acetonitrile was added, *via* a syringe pump, to a solution of freshly distilled  $\text{BF}_3 \cdot \text{Et}_2\text{O}$  in dry acetonitrile. Complete decomposition occurred in less than 30 minutes from the end of the addition. The products obtained were purified by silica gel flash chromatography and characterized.

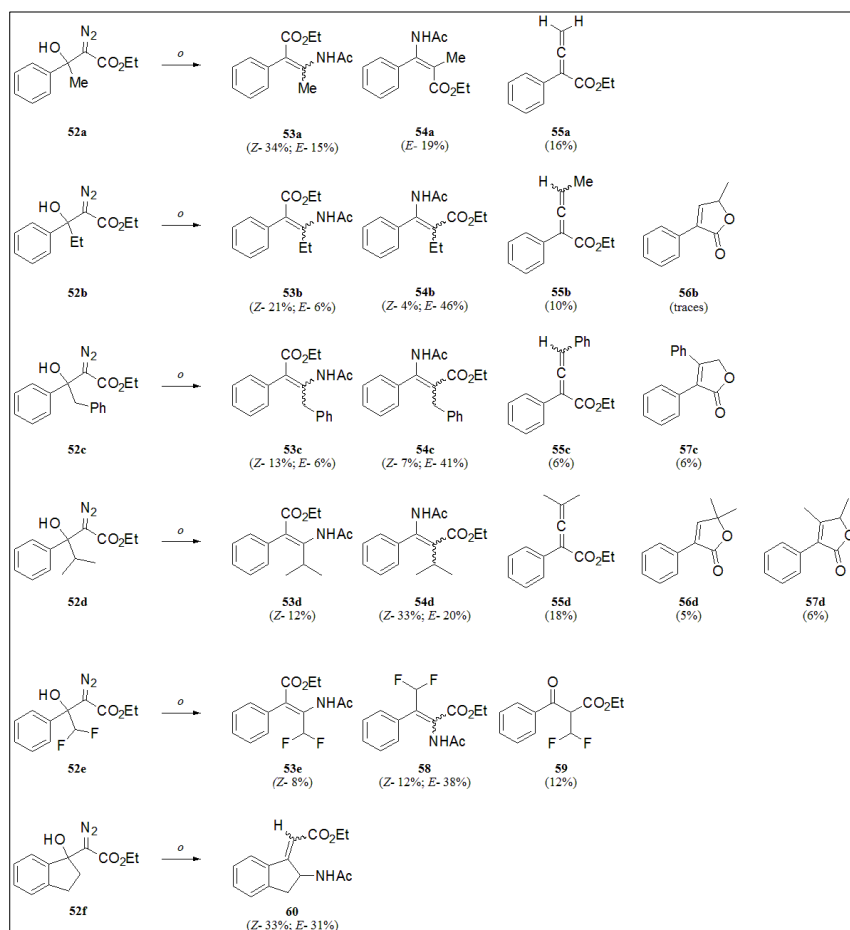
Entry	Substrate	Conditions	Product	Isolated yield
1		A		87%
2		A		91%
3		B		82%
4		B		76%
5		C		80%
6		B		71%

**Table 5.** Aldol type condensation reaction between EDA and different acetophenones presented in this work.

## Results

The reaction of  $\text{BF}_3 \cdot \text{Et}_2\text{O}$  with  $\alpha$ -diazo- $\beta$ -hydroxy- $\beta$ -alkylester **52a** led to the formation of four products, that after purification by silica gel flash chromatography were characterized by mono- and bi-dimensional NMR spectroscopy. To the less polar compound, obtained in 16% isolated yield, was attributed the structure of the unexpected allene derivative **55a** (Scheme 17). Following the polarity ranking order, three out of the four possible isomeric  $\beta$ -enamino esters, *E*-, *Z*-**53a** and *E*-**54a** were isolated.

A similar trend was observed when the ethyl, benzyl and isopropyl derivatives **52b-d** were exposed to  $\text{BF}_3 \cdot \text{Et}_2\text{O}$ . Thus, beside the allene derivatives **55b-d** and lactones **56b**, **56d** and/or **57c-d** (both obtained in moderate yield) the isomeric  $\beta$ -enamino esters, **53b-d** and **54b-d** were obtained as the main reaction products. Unfortunately it has not been possible to isolate pure allene **55c**. Although after flash chromatography the TLC of the pure fractions clearly indicated the presence of pure **55c**, when the solvent was removed *in vacuo*, even at low temperature, the fully conjugated allene **55c** underwent in moderate polymerization.



**Scheme 17.** Summary of the products obtained from decomposition of diazo compounds **52a-f**. Reagents and conditions: *o*)  $\text{BF}_3 \cdot \text{Et}_2\text{O}$ ,  $\text{CH}_3\text{CN}$ , r. t., 30 minutes.



Regarding the  $\text{BF}_3 \cdot \text{Et}_2\text{O}$ -promoted decomposition of the highly reactive ethyl 2-diazo-4,4-difluoro-3-hydroxy-3-phenylbutanoate (**52e**), four different products have been obtained: a *E/Z* couple of  $\alpha$ -enamino ester **58**, the  $\beta$ -enamino ester ethyl (2*Z*)-3-(acetylamino)-4,4-difluoro-2-phenylbut-2-enoate (**53e**) and a minor amount of ethyl 2-benzoyl-3,3-difluoropropanoate (**59**).

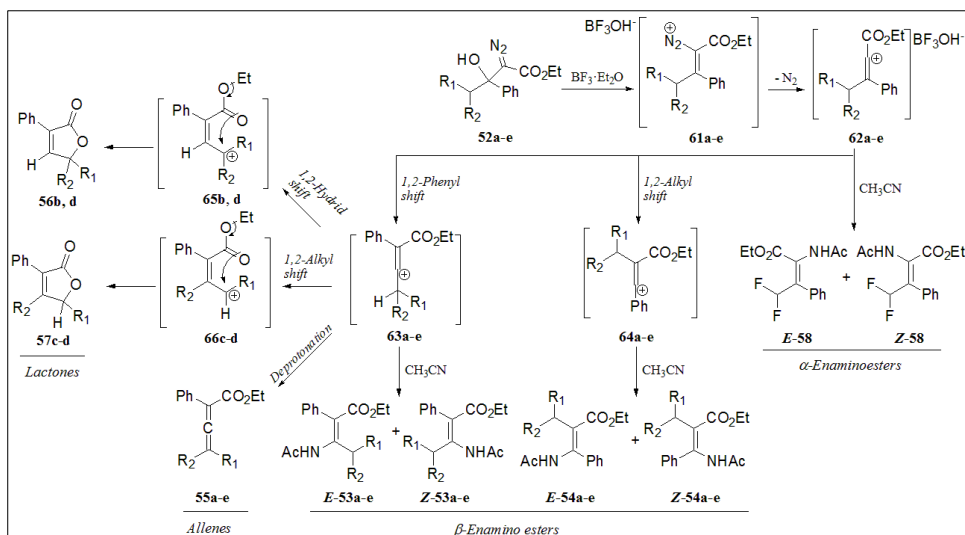
The reaction of the cyclic diazo precursor **52f** with  $\text{BF}_3 \cdot \text{Et}_2\text{O}$  in acetonitrile followed a different reaction pathway. Indeed, the unusual *E/Z* isomeric couple of  $\gamma$ -enamino esters **60** was obtained as the sole traceable reaction product.

### Mechanistic aspects

As previously reported for the decomposition of  $\alpha$ -diazo- $\beta$ -hydroxy esters with  $\text{BF}_3 \cdot \text{Et}_2\text{O}$ , the reaction proceeds *via* prior complexation of the Lewis acid with the OH group (Scheme 18). This is followed by the formation of the alkenyl diazonium salts **61a-e** and nitrogen loss, resulting in the formation of the crucial vinyl cation intermediates **62a-e**. This cation could be either trapped by acetonitrile or undergo in rearrangement pathways, affording the corresponding  $\alpha$ -enamino esters **58** in the first case.

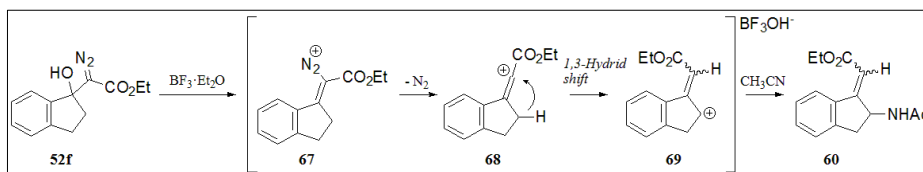
The 1,2-alkyl shift from the vinyl cations **62a-e** results in cations **64a-e** that, when trapped by acetonitrile, afford the corresponding  $\beta$ -enamino ester isomers **54a-e**. Conversely, the 1,2-phenyl shift from **62a-e** generates the corresponding cations **63a-e**. At this stage four different pathways can be envisaged from the vinyl cations **63a-e**: a) solvent trapping, affording  $\beta$ -enamino ester derivatives **53a-e**; b)  $\text{BF}_3\text{OH}^-$ -mediated deprotonation of

the proton  $\alpha$ -located to the vinyl cation, followed by the formation of the additional double bond, resulting in the production of the corresponding allenes **55a-e**; c) 1,2-hydrid shift, leading to the formation of allyl cations **65b** and **65d**, followed by intramolecular cyclization with the adjacent carboxyl function, resulting in the formation of lactones **56b** and **56d**; d) formation of lactones **57c-d**, via a cation cascade analogue to that described in path *c*, involving the 1,2-alkyl shift, formation of the allyl cations **66c-d** and intramolecular cyclization.



**Scheme 18.** Proposed mechanisms for vinyl cations rearrangement cascades.

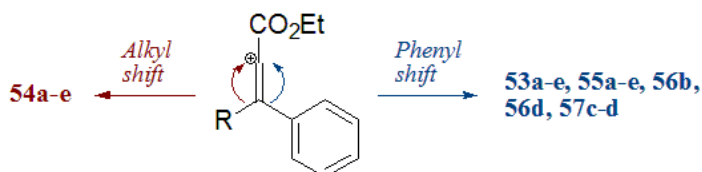
Vinyl cation **68**, generated from the cyclic diazo precursor **52f** (Scheme 19), seems to follow a different pathway, where the formation of the isomeric  $\gamma$ -enamino esters **60** could be explained by the 1,3-hydrid shift, followed by solvent trapping of the intermediate allyl cation **69**.



**Scheme 19.** Proposed mechanism for the formation of **60**.

### Effect of the 3-substituents on product distribution

Analysing the relative yields of formation of different products, it is possible to consider the electronic properties of substituents at position C<sub>3</sub> as the driving force, influencing vinyl cations stabilization/destabilization and propensity for 1,2-alkyl or 1,2-phenyl shift cascades.



Entry	R	Alkyl shift yield	Phenyl shift combined yields
1	Me	19%	65%
2	Et	50%	37%
3	Bn	48%	31%
4	<i>i</i> Pr	53%	41%
5	CHF <sub>2</sub>	-	8%

**Table 6.** Comparison between 1,2-alkyl and 1,2-phenyl shift, and their relationships with C<sub>3</sub> alkyl substituents.

Phenyl shift resulted to be favoured only in the methyl derivative **52a** (Table 6, entry 1), while in the electron richer ethyl, benzyl and isopropyl derivatives **52b-d** the alkyl shift was the dominant process, with a product distribution that seems to follow the electron density of the moiety itself (Bn < Et < *i*Pr).

Regarding cations cascade resulting from vinyl cation **62e**, derived from di-fluorinated precursor **52e**, the formation of both intermediates **62e** and **63e** (Scheme 18) appears highly unfavoured, due to the presence of electron withdrawing groups (CO<sub>2</sub>Et and CHF<sub>2</sub>, respectively)  $\alpha$ -located to the vinyl cation, in both structures. Thus, formation of intermediate **64e**, deriving from 1,2-alkyl shift of the difluoromethyl moiety, should be favoured. However, the poor migratory attitude of CHF<sub>2</sub> group represents a strong drawback for this process and the unusual  $\alpha$ -enamino esters **58**, arisen from direct solvent trapping of **62e**, were obtained as the main reaction products.

### Conclusions

In conclusion, my work has shown that aldol type condensation of EDA and carbonyl compounds can be finely tuned, in order to obtain high yields of the corresponding  $\alpha$ -diazo- $\beta$ -hydroxyesters, bearing different alkyl substituents.

Additionally, results obtained, together with previous reports, contribute to increase the knowledge about the mechanisms sustaining the “ $\alpha$ -diazo- $\beta$ -hydroxyesters/Lewis acid” generation of highly destabilized vinyl cations. The diverse paths of the  $\alpha$ -carbonyl vinyl cations rearrangement cascade can be ascribed to the balance between the migratory attitude and the electronic stabilization/destabilization effects exerted by both  $\alpha$ - and  $\beta$ -substituents.

Further, BF<sub>3</sub>·Et<sub>2</sub>O-induced decomposition of  $\alpha$ -diazo- $\beta$ -hydroxyesters in acetonitrile represents a powerful and versatile method for the synthesis of highly diversified precursors of interesting non-natural amino acids. For future expansion of the scope of this reaction, it would be interesting to

investigate the possibility to apply asymmetric methodologies for the reduction of the double bond of  $\alpha$ -,  $\beta$ - and  $\gamma$ -enamino esters obtained, reasonably by the use of chiral auxiliaries and catalysts, with the aim to obtain optically active  $\alpha$ -,  $\beta$ - and  $\gamma$ -amino acids.

## Section 9. EXPERIMENTAL SECTION (II)

### 9.1. Materials and methods

All reactions were performed *via* classical synthetic procedures, under nitrogen atmosphere, using distilled solvents, at the University of Perugia.

Products were characterized by  $^1\text{H}$ -NMR (mono- and bi-dimensional experiments),  $^{13}\text{C}$ -NMR spectra and GC/MS analyses. Data from characterization are not reported in this section. Please feel free to contact me *via* email if necessary (gianpaolo.vallerini@nemo.unipr.it).

Flash chromatography was performed on Merck silica gel (0.040-0.063 mm), using a Biotage SP1 HPCF separation module. Both 25+M (25 mm x 15.0 cm, 40 g) and 12+M (12 mm x 15.0 cm, 9.0 g) cartridges were used depending on the reaction scale.

$^1\text{H}$ -NMR spectra were recorded at 400 MHz;  $^{13}\text{C}$ -NMR spectra were recorded at 100.6 MHz.

The method EVAL (furnished with the software Enhanced ChemStation Agilent Technology) was used to generate the gradient temperature in the GC-MS analyses.

## 9.2. Synthetic procedures

*General procedure for the preparation of ethyl 2-diazo-3-hydroxycarboxylates (m).*

A cooled (-78 °C) solution of lithium diisopropylamide [LDA, prepared by the addition of *n*-butyllithium, 2.5 M in hexanes (1.20 eq.) to a solution of diisopropylamine (1.40 eq.) in dry THF (2 ml/mmol Bu-Li)] was added in 30 minutes to a stirred solution of the appropriate ketone (1.00 eq.) and ethyl diazoacetate (EDA, 1.10 eq.) in dry THF (2.5 ml/mmol ketone) at -78 °C. The mixture was allowed to stir at -78 °C for 2 hours, at which time the reaction was quenched with saturated aqueous NH<sub>4</sub>Cl (for **51a-b**) or a solution of acetic acid (1.5 ml) in THF (30 ml, for **51c-d** and **51f**) and extracted with ether. The combined organic extracts were washed with saturated aqueous NaHCO<sub>3</sub> and brine, dried over anhydrous Na<sub>2</sub>SO<sub>4</sub>, filtered and concentrated under reduced pressure. The crude residue was purified by filtration on a pad of alumina eluting with hexane/ethyl acetate, 9/1, affording target products in 71-91% yield, as yellow oils.

Ethyl 2-diazo-3-hydroxy-3-difluoromethyl-3-phenylpropanoate (**52e**).

To a stirred solution of LDA (1.50 eq., prepared according to the method cited in the above reaction), a cooled (-78 °C) solution of ethyl diazoacetate (1.20 eq.) in dry THF (2.5 ml/mmol) was added at -78 °C in 15 minutes. After 10 minutes from the end of the addition, a THF (5 ml/mmol) solution of ketone **51e** (1.00 eq.) was added in 10 min at -78 °C. After 15 minutes, a cooled (-78 °C) solution of acetic acid (1.5 ml) in dry THF (30 ml) was added in 5 minutes. The reaction mixture was taken into water and extracted with ether. The combined organic extracts were washed with saturated aqueous NaHCO<sub>3</sub> and brine, dried over anhydrous

Na<sub>2</sub>SO<sub>4</sub>, filtered and concentrated under reduced pressure. The crude residue was purified by filtration on a pad of alumina eluting with petroleum ether/ethyl acetate, 9/1, affording **52e** in 80% yield, as a yellow oil.

*General procedure for the decomposition of ethyl 2-diazo-3-hydroxy-3-phenyl-3-alkylpropanoates **52a-f** (o).*

To a magnetically stirred solution of freshly distilled BF<sub>3</sub>·Et<sub>2</sub>O (1.50 eq.) in dry acetonitrile (5 ml/mmol) was added a solution of  $\alpha$ -diazo- $\beta$ -hydroxyester **52a-f** (1.00 mmol) in dry acetonitrile (30 ml/mmol) with a syringe-pump (0.02 mmol/min) at room temperature. After the end of the addition, the reaction mixture was stirred for additional 30 minutes at room temperature and then poured into saturated aqueous NaHCO<sub>3</sub>, extracted with ethyl acetate, dried over anhydrous Na<sub>2</sub>SO<sub>4</sub>, filtered and concentrated under reduced pressure. The crude residue was purified by silica gel flash chromatography eluting with appropriate gradient of petroleum ether/ethyl acetate mixtures.



## References

- (1) Watkins, J. C.; Jane, D. E. The glutamate story. *British Journal of Pharmacology* **2006**, *147 Suppl 1*, S100–108.
- (2) Platt, S. R. The role of glutamate in central nervous system health and disease – A review. *The Veterinary Journal* **2007**, *173*, 278–286.
- (3) Javitt, D. C.; Schoepp, D.; Kalivas, P. W.; Volkow, N. D.; Zarate, C.; Merchant, K.; Bear, M. F.; Umbricht, D.; Hajos, M.; Potter, W. Z.; Lee, C.-M. Translating Glutamate: From Pathophysiology to Treatment. *Science Translational Medicine* **2011**, *3*, 102mr2.
- (4) Foster, A.; Kemp, J. Glutamate- and GABA-based CNS therapeutics. *Current Opinion in Pharmacology* **2006**, *6*, 7–17.
- (5) Hynd, M. R.; Scott, H. L.; Dodd, P. R. Glutamate-mediated excitotoxicity and neurodegeneration in Alzheimer's disease. *Neurochemistry International* **2004**, *45*, 583–595.
- (6) André, V. M.; Cepeda, C.; Levine, M. S. Dopamine and Glutamate in Huntington's Disease: A Balancing Act. *CNS Neuroscience & Therapeutics* **2010**, *16*, 163–178.
- (7) Bowie, D. Ionotropic glutamate receptors & CNS disorders. *CNS & Neurological Disorders Drug Targets* **2008**, *7*, 129–143.
- (8) Traynelis, S. F.; Wollmuth, L. P.; McBain, C. J.; Menniti, F. S.; Vance, K. M.; Ogden, K. K.; Hansen, K. B.; Yuan, H.; Myers, S. J.; Dingledine, R. Glutamate Receptor Ion Channels: Structure, Regulation, and Function. *Pharmacological Reviews* **2010**, *62*, 405–496.
- (9) Cull-Candy, S.; Brickley, S.; Farrant, M. NMDA receptor subunits: diversity, development and disease. *Current Opinion in Neurobiology* **2001**, *11*, 327–335.
- (10) Chang, P.; Verbich, D.; McKinney, R. AMPA receptors as drug targets in neurological disease—advantages, caveats, and future outlook. *The European Journal of Neuroscience* **2012**, *35*, 1908–1916.
- (11) Rodríguez-Moreno, A.; Sihra, T. S. Metabotropic actions of kainate receptors in the control of glutamate release in the hippocampus. *Advances in Experimental Medicine and Biology* **2011**, *717*, 39–48.
- (12) Erreger, K.; Chen, P. E.; Wyllie, D. J. A.; Traynelis, S. F. Glutamate receptor gating. *Critical Reviews in Neurobiology* **2004**, *16*, 187–224.
- (13) Sanz-Clemente, A.; Nicoll, R. A.; Roche, K. W. Diversity in NMDA Receptor Composition: Many Regulators, Many Consequences. *Neuroscientist* **2013**, *19*, 62–75.
- (14) Wolosker, H.; Dumin, E.; Balan, L.; Foltyn, V. N. D-amino acids in the brain: D-serine in neurotransmission and neurodegeneration. *The FEBS journal* **2008**, *275*, 3514–3526.

- (15) Niswender, C. M.; Conn, P. J. Metabotropic glutamate receptors: physiology, pharmacology, and disease. *Annual Review of Pharmacology and Toxicology* **2010**, *50*, 295–322.
- (16) Quibell, R.; Prommer, E. E.; Mihalyo, M.; Twycross, R.; Wilcock, A. Ketamine\*. *Journal of Pain and Symptom Management* **2011**, *41*, 640–649.
- (17) Robinson, D. M.; Keating, G. M. Memantine: a review of its use in Alzheimer's disease. *Drugs* **2006**, *66*, 1515–1534.
- (18) Landmark, C. J. Targets for antiepileptic drugs in the synapse. *Medical Science Monitor: International Medical Journal of Experimental and Clinical Research* **2007**, *13*, RA1–7.
- (19) Curtis, D. R.; Watkins, J. C. The Excitation and Depression of Spinal Neurones by Structurally Related Amino Acids. *Journal of Neurochemistry* **1960**, *6*, 117–141.
- (20) Stewart, C. N.; Coursin, D. B.; Bhagavan, H. N. Electroencephalographic study of l-glutamate induced seizures in rats. *Toxicology and Applied Pharmacology* **1972**, *23*, 635–639.
- (21) Schwarcz, R.; Pellicciari, R. Manipulation of brain kynurenines: glial targets, neuronal effects, and clinical opportunities. *The Journal of Pharmacology and Experimental Therapeutics* **2002**, *303*, 1–10.
- (22) Schwarcz, R. The kynurenine pathway of tryptophan degradation as a drug target. *Current Opinion in Pharmacology* **2004**, *4*, 12–17.
- (23) Costantino, G. New promises for manipulation of kynurenine pathway in cancer and neurological diseases. *Expert Opinion on Therapeutic Targets* **2009**, *13*, 247–258.
- (24) Schwarcz, R.; Bruno, J.; Muchowski, P.; Wu, H.-Q. Kynurenines in the mammalian brain: when physiology meets pathology. *Nature Reviews. Neuroscience* **2012**, *13*, 465–477.
- (25) Stone, T.; Forrest, C.; Darlington, L. Kynurenine pathway inhibition as a therapeutic strategy for neuroprotection. *The FEBS journal* **2012**, *279*, 1386–1397.
- (26) Guillemín, G. J.; Cullen, K. M.; Lim, C. K.; Smythe, G. A.; Garner, B.; Kapoor, V.; Takikawa, O.; Brew, B. J. Characterization of the Kynurenine Pathway in Human Neurons. *The Journal of Neuroscience* **2007**, *27*, 12884–12892.
- (27) Leklem, J. E. Quantitative aspects of tryptophan metabolism in humans and other species: a review. *The American Journal of Clinical Nutrition* **1971**, *24*, 659–672.
- (28) Thomas, S. R.; Stocker, R. Redox reactions related to indoleamine 2,3-dioxygenase and tryptophan metabolism along the kynurenine pathway. *Redox Report* **1999**, *4*, 199–220.
- (29) Ball, H. J.; Yuasa, H. J.; Austin, C. J. D.; Weiser, S.; Hunt, N. H. Indoleamine 2,3-dioxygenase-2; a new enzyme in the kynurenine pathway. *The International Journal of Biochemistry & Cell Biology* **2009**, *41*, 467–471.

- (30) Ren S.; Correia M.A. Heme: A Regulator of Rat Hepatic Tryptophan 2,3-Dioxygenase? *Archives of Biochemistry and Biophysics* **2000**, *377*, 195–203.
- (31) Dang, Y.; Dale, W. E.; Brown, O. R. Comparative effects of oxygen on indoleamine 2,3-dioxygenase and tryptophan 2,3-dioxygenase of the kynurenine pathway. *Free Radical Biology and Medicine* **2000**, *28*, 615–624.
- (32) Speciale, C.; Schwarcz, R. Uptake of Kynurenine into Rat Brain Slices. *Journal of Neurochemistry* **1990**, *54*, 156–163.
- (33) Amori, L.; Guidetti, P.; Pellicciari, R.; Kajii, Y.; Schwarcz, R. On the relationship between the two branches of the kynurenine pathway in the rat brain in vivo. *Journal of Neurochemistry* **2009**, *109*, 316–325.
- (34) Guidetti, P.; Hoffman, G. E.; Melendez-Ferro, M.; Albuquerque, E. X.; Schwarcz, R. Astrocytic localization of kynurenine aminotransferase II in the rat brain visualized by immunocytochemistry. *Glia* **2007**, *55*, 78–92.
- (35) Han, Q.; Cai, T.; Tagle, D. A.; Li, J. Structure, expression, and function of kynurenine aminotransferases in human and rodent brains. *Cellular and Molecular Life Sciences* **2009**, *67*, 353–368.
- (36) Chiarugi, A.; Carpenedo, R.; Molina, M. T.; Mattoli, L.; Pellicciari, R.; Moroni, F. Comparison of the Neurochemical and Behavioral Effects Resulting from the Inhibition of Kynurenine Hydroxylase and/or Kynureninase. *Journal of Neurochemistry* **1995**, *65*, 1176–1183.
- (37) Copeland, C. S.; Neale, S. A.; Salt, T. E. Actions of Xanthurenic Acid, a putative endogenous Group II metabotropic glutamate receptor agonist, on sensory transmission in the thalamus. *Neuropharmacology* **2013**, *66*, 133–142.
- (38) Kawai, J.; Okuno, E.; Kido, R. Organ distribution of rat kynureninase and changes of its activity during development. *Enzyme* **1988**, *39*, 181–189.
- (39) Baran, H.; Schwarcz, R. Presence of 3-Hydroxyanthranilic Acid in Rat Tissues and Evidence for Its Production from Anthranilic Acid in the Brain. *Journal of Neurochemistry* **1990**, *55*, 738–744.
- (40) Fazio, F.; Lionetto, L.; Molinaro, G.; Bertrand, H.; Acher, F.; Ngomba, R.; Notartomaso, S.; Curini, M.; Rosati, O.; Scarselli, P.; Di Marco, R.; Battaglia, G.; Bruno, V.; Simmaco, M.; Pin, J.; Nicoletti, F.; Goudet, C. Cinnabarinic acid, an endogenous metabolite of the kynurenine pathway, activates type 4 metabotropic glutamate receptors. *Molecular Pharmacology* **2012**, *81*, 643–656.
- (41) Malherbe, P.; Köhler, C.; Da Prada, M.; Lang, G.; Kiefer, V.; Schwarcz, R.; Lahm, H. W.; Cesura, A. M. Molecular cloning and functional expression of human 3-hydroxyanthranilic-acid dioxygenase. *The Journal of Biological Chemistry* **1994**, *269*, 13792–13797.
- (42) Pucci, L.; Perozzi, S.; Cimadamore, F.; Orsomando, G.; Raffaelli, N. Tissue expression

and biochemical characterization of human 2-amino 3-carboxymuconate 6-semialdehyde decarboxylase, a key enzyme in tryptophan catabolism. *The FEBS Journal* **2007**, *274*, 827–840.

(43) Foster, A. C.; Zinkand, W. C.; Schwarcz, R. Quinolinic Acid Phosphoribosyltransferase in Rat Brain. *Journal of Neurochemistry* **1985**, *44*, 446–454.

(44) Turski, W. A.; Nakamura, M.; Todd, W. P.; Carpenter, B. K.; Whetsell Jr., W. O.; Schwarcz, R. Identification and quantification of kynurenic acid in human brain tissue. *Brain Research* **1988**, *454*, 164–169.

(45) Perkins, M. N.; Stone, T. W. An iontophoretic investigation of the actions of convulsant kynurenines and their interaction with the endogenous excitant quinolinic acid. *Brain Research* **1982**, *247*, 184–187.

(46) Parsons, C. G.; Danysz, W.; Quack, G.; Hartmann, S.; Lorenz, B.; Wollenburg, C.; Baran, L.; Przegalinski, E.; Kostowski, W.; Krzascik, P.; Chizh, B.; Headley, P. M. Novel systemically active antagonists of the glycine site of the N-methyl-D-aspartate receptor: electrophysiological, biochemical and behavioral characterization. *The Journal of Pharmacology and Experimental Therapeutics* **1997**, *283*, 1264–1275.

(47) Lugo-Huitrón, R.; Blanco-Ayala, T.; Ugalde-Muñiz, P.; Carrillo-Mora, P.; Pedraza-Chaverri, J.; Silva-Adaya, D.; Maldonado, P. D.; Torres, I.; Pinzón, E.; Ortiz-Islas, E.; López, T.; García, E.; Pineda, B.; Torres-Ramos, M.; Santamaría, A.; La Cruz, V. P.-D. On the antioxidant properties of kynurenic acid: free radical scavenging activity and inhibition of oxidative stress. *Neurotoxicology and Teratology* **2011**, *33*, 538–547.

(48) Hilmas, C.; Pereira, E. F. R.; Alkondon, M.; Rassoulpour, A.; Schwarcz, R.; Albuquerque, E. X. The Brain Metabolite Kynurenic Acid Inhibits  $\alpha 7$  Nicotinic Receptor Activity and Increases Non- $\alpha 7$  Nicotinic Receptor Expression: Physiopathological Implications. *The Journal of Neuroscience* **2001**, *21*, 7463–7473.

(49) Wu, H.-Q.; Pereira, E.; Bruno, J.; Pellicciari, R.; Albuquerque, E.; Schwarcz, R. The astrocyte-derived  $\alpha 7$  nicotinic receptor antagonist kynurenic acid controls extracellular glutamate levels in the prefrontal cortex. *Journal of Molecular Neuroscience* **2010**, *40*, 204–210.

(50) Giles, G. I.; Collins, C. A.; Stone, T. W.; Jacob, C. Electrochemical and in vitro evaluation of the redox-properties of kynurenine species. *Biochemical and Biophysical Research Communications* **2003**, *300*, 719–724.

(51) Stone, T. W.; Perkins, M. N. Quinolinic acid: A potent endogenous excitant at amino acid receptors in CNS. *European Journal of Pharmacology* **1981**, *72*, 411–412.

(52) Lapin, I. P. Stimulant and convulsive effects of kynurenines injected into brain ventricles in mice. *Journal of Neural Transmission* **1978**, *42*, 37–43.

(53) Prado De Carvalho, L.; Bochet, P.; Rossier, J. The endogenous agonist quinolinic acid and the non endogenous homoquinolinic acid discriminate between NMDAR2 receptor subunits.

*Neurochemistry International* **1996**, 28, 445–452.

(54) Miranda, A. .; Sutton, M. .; Beninger, R. .; Jhamandas, K.; Boegman, R. . Quinolinic acid lesion of the nigrostriatal pathway: effect on turning behaviour and protection by elevation of endogenous kynurenic acid in *rattus norvegicus*. *Neuroscience Letters* **1999**, 262, 81–84.

(55) Tkáč, I.; Keene, C. D.; Pfeuffer, J.; Low, W. C.; Gruetter, R. Metabolic changes in quinolinic acid-lesioned rat striatum detected non-invasively by in vivo <sup>1</sup>H NMR spectroscopy. *Journal of Neuroscience Research* **2001**, 66, 891–898.

(56) Tattersfield, A. S.; Croon, R. J.; Liu, Y. W.; Kells, A. P.; Faull, R. L.; Connor, B. Neurogenesis in the striatum of the quinolinic acid lesion model of Huntington's disease. *Neuroscience* **2004**, 127, 319–32.

(57) Chugani, D. C.  $\alpha$ -methyl-l-tryptophan: mechanisms for tracer localization of epileptogenic brain regions. *Biomarkers in Medicine* **2011**, 5, 567–575.

(58) Guillemín, G. J.; Brew, B. J.; Noonan, C. E.; Takikawa, O.; Cullen, K. M. Indoleamine 2,3 dioxygenase and quinolinic acid Immunoreactivity in Alzheimer's disease hippocampus. *Neuropathology and Applied Neurobiology* **2005**, 31, 395–404.

(59) Zádori, D.; Klivényi, P.; Toldi, J.; Fülöp, F.; Vécsei, L. Kynurenines in Parkinson's disease: therapeutic perspectives. *Journal of Neural Transmission* **2012**, 119, 275–283.

(60) Sardar, A. M.; Bell, J. E.; Reynolds, G. P. Increased Concentrations of the Neurotoxin 3-Hydroxykynurenine in the Frontal Cortex of HIV-1-Positive Patients. *Journal of Neurochemistry* **1995**, 64, 932–935.

(61) Chen, Y.; Stankovic, R.; Cullen, K. M.; Meininger, V.; Garner, B.; Coggan, S.; Grant, R.; Brew, B. J.; Guillemín, G. J. The Kynurenine Pathway and Inflammation in Amyotrophic Lateral Sclerosis. *Neurotoxicity Research* **2010**, 18, 132–142.

(62) Lim, C.; Brew, B.; Sundaram, G.; Guillemín, G. Understanding the roles of the kynurenine pathway in multiple sclerosis progression. *International Journal of Tryptophan Research* **2010**, 3, 157–167.

(63) Giorgini, F.; Guidetti, P.; Nguyen, Q.; Bennett, S.; Muchowski, P. A genomic screen in yeast implicates kynurenine 3-monooxygenase as a therapeutic target for Huntington disease. *Nature Genetics* **2005**, 37, 526–531.

(64) Ha, A. D.; Fung, V. S. C. Huntington's disease. *Current Opinion in Neurology* **2012**, 25, 491–498.

(65) Tai, Y. F.; Pavese, N.; Gerhard, A.; Tabrizi, S. J.; Barker, R. A.; Brooks, D. J.; Piccini, P. Microglial activation in presymptomatic Huntington's disease gene carriers. *Brain: a Journal of Neurology* **2007**, 130, 1759–1766.

(66) Guidetti, P.; Luthi-Carter, R. E.; Augood, S. J.; Schwarcz, R. Neostriatal and cortical

quinolinate levels are increased in early grade Huntington's disease. *Neurobiology of Disease* **2004**, *17*, 455–461.

(67) Slow, E. J.; Raamsdonk, J. van; Rogers, D.; Coleman, S. H.; Graham, R. K.; Deng, Y.; Oh, R.; Bissada, N.; Hossain, S. M.; Yang, Y.-Z.; Li, X.-J.; Simpson, E. M.; Gutekunst, C.-A.; Leavitt, B. R.; Hayden, M. R. Selective striatal neuronal loss in a YAC128 mouse model of Huntington disease. *Human Molecular Genetics* **2003**, *12*, 1555–1567.

(68) Mándi, Y.; Vécsei, L. The kynurenine system and immunoregulation. *Journal of Neural Transmission* **2012**, *119*, 197–209.

(69) Sandyk, R. Tryptophan Availability and the Susceptibility to Stress in Multiple Sclerosis: A Hypothesis. *International Journal of Neuroscience* **1996**, *86*, 47–53.

(70) Hartai, Z.; Klivenyi, P.; Janaky, T.; Penke, B.; Dux, L.; Vecsei, L. Kynurenine metabolism in multiple sclerosis. *Acta Neurologica Scandinavica* **2005**, *112*, 93–96.

(71) Rejdak, K.; Bartosik-Psujek, H.; Dobosz, B.; Kocki, T.; Grieb, P.; Giovannoni, G.; Turski, W. A.; Stelmasiak, Z. Decreased level of kynurenic acid in cerebrospinal fluid of relapsing-onset multiple sclerosis patients. *Neuroscience Letters* **2002**, *331*, 63–65.

(72) Benveniste, E. N. Role of macrophages/microglia in multiple sclerosis and experimental allergic encephalomyelitis. *Journal of Molecular Medicine* **1997**, *75*, 165–173.

(73) Braidy, N.; Grant, R.; Brew, B. J.; Adams, S.; Jayasena, T.; Guillemin, G. J. Effects of Kynurenine Pathway Metabolites on Intracellular NAD<sup>+</sup> Synthesis and Cell Death in Human Primary Astrocytes and Neurons. *International Journal of Tryptophan Research* **2009**, *2*, 61–69.

(74) Cammer, W. Oligodendrocyte killing by quinolinic acid in vitro. *Brain Research* **2001**, *896*, 157–160.

(75) Kwidzinski, E.; Bunse, J.; Aktas, O.; Richter, D.; Mutlu, L.; Zipp, F.; Nitsch, R.; Bechmann, I. Indolamine 2,3-dioxygenase is expressed in the CNS and down-regulates autoimmune inflammation. *The FASEB Journal* **2005**.

(76) Flanagan, E. M.; Erickson, J. B.; Viveros, O. H.; Chang, S. Y.; Reinhard, J. F. Neurotoxin Quinolinic Acid Is Selectively Elevated in Spinal Cords of Rats with Experimental Allergic Encephalomyelitis. *Journal of Neurochemistry* **1995**, *64*, 1192–1196.

(77) Chiarugi, A.; Cozzi, A.; Ballerini, C.; Massacesi, L.; Moroni, F. Kynurenine 3-mono-oxygenase activity and neurotoxic kynurenine metabolites increase in the spinal cord of rats with experimental allergic encephalomyelitis. *Neuroscience* **2001**, *102*, 687–695.

(78) Kurnasov, O.; Goral, V.; Colabroy, K.; Gerdes, S.; Anantha, S.; Osterman, A.; Begley, T. P. NAD Biosynthesis: Identification of the Tryptophan to Quinolinate Pathway in Bacteria. *Chemistry & Biology* **2003**, *10*, 1195–1204.

- (79) Colabroy, K.; Zhai, H.; Li, T.; Ge, Y.; Zhang, Y.; Liu, A.; Ealick, S.; McLafferty, F.; Begley, T. The mechanism of inactivation of 3-hydroxyanthranilate-3,4-dioxygenase by 4-chloro-3-hydroxyanthranilate. *Biochemistry* **2005**, *44*, 7623–7631.
- (80) Zhang, Y.; Colabroy, K.; Begley, T.; Ealick, S. Structural studies on 3-hydroxyanthranilate-3,4-dioxygenase: the catalytic mechanism of a complex oxidation involved in NAD biosynthesis. *Biochemistry* **2005**, *44*, 7632–7643.
- (81) Đilović, I.; Gliubich, F.; Malpeli, G.; Zanotti, G.; Matković-Čalogović, D. Crystal structure of bovine 3-hydroxyanthranilate 3,4-dioxygenase. *Biopolymers* **2009**, *91*, 1189–1195.
- (82) Li, X.; Guo, M.; Fan, J.; Tang, W.; Wang, D.; Ge, H.; Rong, H.; Teng, M.; Niu, L.; Liu, Q.; Hao, Q. Crystal structure of 3-hydroxyanthranilic acid 3,4-dioxygenase from *Saccharomyces cerevisiae*: A special subgroup of the type III extradiol dioxygenases. *Protein Science: A Publication of the Protein Society* **2006**, *15*, 761–773.
- (83) Dunwell, J. M.; Purvis, A.; Khuri, S. Cupins: the most functionally diverse protein superfamily? *Phytochemistry* **2004**, *65*, 7–17.
- (84) Bugg, T. D. Oxygenases: mechanisms and structural motifs for O(2) activation. *Current Opinion in Chemical Biology* **2001**, *5*, 550–5.
- (85) Parli, C. J.; Krieter, P.; Schmidt, B. Metabolism of 6-chlorotryptophan to 4-chloro-3-hydroxyanthranilic acid: A potent inhibitor of 3-hydroxyanthranilic acid oxidase. *Archives of Biochemistry and Biophysics* **1980**, *203*, 161–166.
- (86) Todd, W. P.; Carpenter, B. K. Preparation of 4-Halo-3-Hydroxyanthranilates and Demonstration of their Inhibition of 3-Hydroxyanthranilate Oxygenase Activity in Rat and Human Brain Tissue. *Preparative Biochemistry* **1989**, *19*, 155–165.
- (87) Linderberg, M.; Hellberg, S.; Björk, S.; Gotthammar, B.; Högberg, T.; Persson, K.; Schwarcz, R.; Luthman, J.; Johansson, R. Synthesis and QSAR of substituted 3-hydroxyanthranilic acid derivatives as inhibitors of 3-hydroxyanthranilic acid dioxygenase (3-HAO). *European Journal of Medicinal Chemistry* **1999**, *34*, 729–744.
- (88) Yates, J. R.; Heyes, M. P.; Blight, A. R. 4-Chloro-3-Hydroxyanthranilate Reduces Local Quinolinic Acid Synthesis, Improves Functional Recovery, and Preserves White Matter after Spinal Cord Injury. *Journal of Neurotrauma* **2006**, *23*, 866–881.
- (89) Luthman, J.; Radesäter, A. C.; Oberg, C. Effects of the 3-hydroxyanthranilic acid analogue NCR-631 on anoxia-, IL-1 beta- and LPS-induced hippocampal pyramidal cell loss in vitro. *Amino Acids* **1998**, *14*, 263–269.
- (90) Luthman, J. Anticonvulsant effects of the 3-hydroxyanthranilic acid dioxygenase inhibitor NCR-631. *Amino Acids* **2000**, *19*.
- (91) Fornstedt-Wallin, B.; Lundström, J.; Fredriksson, G.; Schwarcz, R.; Luthman, J. 3-Hydroxyanthranilic acid accumulation following administration of the 3-hydroxyanthranilic acid

3,4-dioxygenase inhibitor NCR-631. *European Journal of Pharmacology* **1999**, *386*, 15–24.

(92) Connor, T. J.; Starr, N.; O'Sullivan, J. B.; Harkin, A. Induction of indolamine 2,3-dioxygenase and kynurenine 3-monooxygenase in rat brain following a systemic inflammatory challenge: A role for IFN- $\gamma$ ? *Neuroscience Letters* **2008**, *441*, 29–34.

(93) Youssif, S. Recent trends in the chemistry of pyridine N-oxides. *ARKIVOC* **2001**, *i*, 242–268.

(94) Epszajn, J.; Bieniek, A.; Kowalska, J. A. Application of organolithium and related reagents in synthesis. Part 9. Synthesis and metallation of 4-chloropicolin- and 2-chloroisonicotinilides. A useful method for preparation of 2,3,4-trisubstituted pyridines. *Tetrahedron* **1991**, *47*, 1697–1706.

(95) Cartwright, D.; Ferguson, J. R.; Giannopoulos, T.; Varvounis, G.; Wakefield, B. J. Abnormal Nucleophilic Substitution in 3-Trichloromethylpyridine, its N-Oxide and 3,5-Bis(trichloromethyl)pyridine. *Tetrahedron* **1995**, *51*, 12791–12796.

(96) Murray, R. W.; Iyanar, K.; Chen, J.; Wearing, J. T. Methyltrioxorhenium-catalyzed C-H insertion reactions of hydrogen peroxide. *Tetrahedron Letters* **1995**, *36*, 6415–6418.

(97) Murray, R. W.; Iyanar, K.; Chen, J.; Wearing, J. T. Oxidation of organonitrogen compounds by the methyltrioxorhenium-hydrogen peroxide system. *Tetrahedron Letters* **1996**, *37*, 805–808.

(98) Hill, M. D. Recent Strategies for the Synthesis of Pyridine Derivatives. *Chemistry – A European Journal* **2010**, *16*, 12052–12062.

(99) Slobbe, P.; Ruijter, E.; Orru, R. V. A. Recent applications of multicomponent reactions in medicinal chemistry. *MedChemComm* **2012**, *3*, 1189–1218.

(100) Shi, F.; Tu, S.; Fang, F.; Li, T. One-pot synthesis of 2-aminopyridine derivatives under microwave irradiation without solvent. *ARKIVOC* **2005**, *i*, 137–142.

(101) Presser, A.; Hüfner, A. Trimethylsilyldiazomethane A Mild and Efficient Reagent for the Methylation of Carboxylic Acids and Alcohols in Natural Products. *Monatshefte für Chemie / Chemical Monthly* **2004**, *135*, 1015–1022.

(102) Thomas, A. A.; Le Huerou, Y.; De Meese, J.; Gunawardana, I.; Kaplan, T.; Romoff, T. T.; Gonzales, S. S.; Condroski, K.; Boyd, S. A.; Ballard, J.; Bernat, B.; DeWolf, W.; Han, M.; Lee, P.; Lemieux, C.; Pedersen, R.; Pheneger, J.; Poch, G.; Smith, D.; Sullivan, F.; Weiler, S.; Wright, S. K.; Lin, J.; Brandhuber, B.; Vigers, G. Synthesis, in vitro and in vivo activity of thiamine antagonist transketolase inhibitors. *Bioorganic & Medicinal Chemistry Letters* **2008**, *18*, 2206–2210.

(103) Zhang, D.; Sun, H.; Zhang, L.; Zhou, Y.; Li, C.; Jiang, H.; Chen, K.; Liu, H. An expedient Pd/DBU mediated cyanation of aryl/heteroaryl bromides with K<sub>4</sub>[Fe(CN)<sub>6</sub>]. *Chemical*



*Communications* **2012**, *48*, 2909–2911.

(104) Ma, J.-A. Recent Developments in the Catalytic Asymmetric Synthesis of  $\alpha$ - and  $\beta$ -Amino Acids. *Angewandte Chemie International Edition* **2003**, *42*, 4290–4299.

(105) Weiner, B.; Szymański, W.; Janssen, D. B.; Minnaard, A. J.; Feringa, B. L. Recent advances in the catalytic asymmetric synthesis of  $\beta$ -amino acids. *Chemical Society Reviews* **2010**, *39*, 1656–1691.

(106) Wang, J.; Liu, X.; Feng, X. Asymmetric Strecker Reactions. *Chemical Reviews* **2011**, *111*, 6947–6983.

(107) Xiao-Hua, C.; Hui, G.; Bing, X. Recent progress in the asymmetric Mannich reaction. *European Journal of Chemistry* **2012**, *3*, 258–266.

(108) O'Donnell, M. J. The Enantioselective Synthesis of  $\alpha$ -Amino Acids by Phase-Transfer Catalysis with Achiral Schiff Base Esters. *Accounts of Chemical Research* **2004**, *37*, 506–517.

(109) Davis, F. A.; Chen, B.-C. Asymmetric synthesis of amino acids using sulfinimines (thiooxime S-oxides). *Chemical Society Reviews* **1998**, *27*, 13–18.

(110) Xie, J.-H.; Zhu, S.-F.; Zhou, Q.-L. Recent advances in transition metal-catalyzed enantioselective hydrogenation of unprotected enamines. *Chemical Society Reviews* **2012**, *41*, 4126–4139.

(111) Ye, T.; McKerver, M. A. Organic Synthesis with  $\alpha$ -Diazo Carbonyl Compounds. *Chemical Reviews* **1994**, *94*, 1091–1160.

(112) Lee, E. C.; Fu, G. C. Copper-Catalyzed Asymmetric N–H Insertion Reactions: Couplings of Diazo Compounds with Carbamates to Generate  $\alpha$ -Amino Acids. *Journal of the American Chemical Society* **2007**, *129*, 12066–12067.

(113) Koch, K.; Podlech, J. Exceptionally Simple Homologation of Protected  $\alpha$ - to  $\beta$ -Amino Acids in the Presence of Silica Gel. *Synthetic Communications* **2005**, *35*, 2789–2794.

(114) Adams, L. A.; Aggarwal, V. K.; Bonnert, R. V.; Bressel, B.; Cox, R. J.; Shepherd, J.; De Vicente, J.; Walter, M.; Whittingham, W. G.; Winn, C. L. Diastereoselective Synthesis of Cyclopropane Amino Acids Using Diazo Compounds Generated in Situ. *The Journal of Organic Chemistry* **2003**, *68*, 9433–9440.

(115) Pellicciari, R.; Natalini, B.; Sadeghpour, B. M.; Marinozzi, M.; Snyder, J. P.; Williamson, B. L.; Kuethe, J. T.; Padwa, A. The Reaction of  $\alpha$ -Diazo- $\beta$ -hydroxy Esters with Boron Trifluoride Etherate: Generation and Rearrangement of Destabilized Vinyl Cations. A Detailed Experimental and Theoretical Study. *Journal of the American Chemical Society* **1996**, *118*, 1–12.

(116) Gioiello, A.; Venturoni, F.; Natalini, B.; Pellicciari, R. BF(3).Et(2)O-induced decomposition of ethyl 2-diazo-3-hydroxy-3,3-diarylpropanoates in acetonitrile: a novel approach to 2,3-diaryl  $\beta$ -enamino ester derivatives. *The Journal of Organic Chemistry* **2009**, *74*, 3520–

3523.

(117) Nagao, K.; Chiba, M.; Kim, S.-W. A New Efficient Homologation Reaction of Ketones via their Lithiodiazoacetate Adducts. *Synthesis* **1983**, 1983, 197–199.

(118) Draghici, C.; Brewer, M. Lewis acid promoted carbon-carbon bond cleavage of gamma-silyloxy-beta-hydroxy-alpha-diazoesters. *Journal of the American Chemical Society* **2008**, 130, 3766–3767.

(119) Gioiello, A.; Venturoni, F.; Marinozzi, M.; Natalini, B.; Pellicciari, R. Exploring the synthetic versatility of the Lewis acid induced decomposition reaction of  $\alpha$ -diazo- $\beta$ -hydroxy esters. The case of ethyl diazo(3-hydroxy-2-oxo-2,3-dihydro-1H-indol-3-yl)acetate. *The Journal of Organic Chemistry* **2011**, 76, 7431–7437.

(120) Pellicciari, R.; Castagnino, E.; Fringuelli, R.; Corsano, S. The preparation of acylacetylenic derivatives of  $\alpha$ -cyclocitral on route to physiologically active terpenes. *Tetrahedron Letters* **1979**, 20, 481–484.